The historical Greenland Climate Network (GC-Net) curated and augmented Level 1 dataset

Baptiste Vandecrux[1], Jason E. Box[1], Andreas P. Ahlstrøm[1], Signe B. Andersen[1], Nicolas Bayou[2], William T. Colgan[1], Nicolas J. Cullen[3], Robert S. Fausto[1], Dominik Haas-Artho[4], Achim Heilig[5], Derek A. Houtz[4], Penelope How[1], Ionut Iosifescu Enescu[4], Nanna B. Karlsson[1], Rebecca Kurup Buchholz[4], Kenneth D. Mankoff[6,7], Daniel McGrath[8], Noah P. Molotch[9], Bianca Perren[10], Maiken K. Revheim[1], Anja Rutishauser[1], Kevin Sampson[11], Martin Schneebeli[12], Sandy Starkweather[13,14], Simon Steffen[15], Jeff Weber[16], Patrick J. Wright[1], Henry Jay Zwally[17], Konrad Steffen[4,14†]

[1]Department of Glaciology and Climate, Geological Survey of Denmark and Greenland (GEUS), Copenhagen, 1350, Denmark
[2]UNAVCO, Boulder, CO 80301, USA
[3]School of Geography, University of Otago, Dunedin, 9016, New Zealand
[4]Swiss Federal Institute for Forest, Snow and Landscape Research WSL, Birmensdorf, 8903, Switzerland
[5]Department of Earth and Environmental Sciences, Ludwig Maximilian University, Munich, 80539, Germany
[6]Autonomic Integra LLC, New York, NY 10025 USA
[7]NASA Goddard Institute for Space Studies, New York, NY 10025, USA
[8]Department of Geosciences, Colorado State University, Fort Collins, CO 80523, USA
[9]Institute of Arctic and Alpine Research, University of Colorado Boulder, Boulder, CO 80303, USA
[10]British Antarctic Survey, Cambridge, CB3 0ET, UK
[11]National Center for Atmospheric Research, Boulder, Colorado, CO 80305, USA
[12]WSL Institute for Snow and Avalanche Research SLF, Davos, 7260, Switzerland
[13]Cooperative Institute for Research in Environmental Sciences, University of Colorado Boulder, Boulder CO, 80309, USA
[14]National Oceanic and Atmospheric Administration, Boulder, CO 80305, USA
[15]Earthanme, Zürich, 8057, Switzerland
[16]Unidata Program Center, University Corporation for Atmospheric Research, Boulder, CO 80301, USA
[17]Earth System Interdisciplinary Science Center (ESSIC), University of Maryland, College Park, MD 20742, USA
†deceased

Correspondence to: Baptiste Vandecrux (bav@geus.dk)

Abstract. The Greenland Climate Network (GC-Net) consists of 31 automatic weather stations (AWS) at 30 sites across the Greenland Ice Sheet. The first site was initiated in 1990, and the project has operated almost continuously since 1995 under the leadership of the late Prof. Konrad Steffen. The GC-Net AWS measured air temperature, relative humidity, wind speed, atmospheric pressure, downward and reflected shortwave irradiance, net radiation, ice and firn temperatures. The majority of the GC-Net sites were located in the ice sheet accumulation area (17 AWS), while 11 AWS were located in the ablation area and two sites (three AWS) were located close to the equilibrium line altitude. Additionally, three AWS of similar design to the GC-Net AWS were installed by Prof. K. Steffen's team on the Larsen C ice shelf, Antarctica. After more than three decades of operation, the GC-Net AWS are being decommissioned and replaced by new AWS operated by the Geological Survey of Denmark and Greenland (GEUS). Therefore, making a reassessment of the historical GC-Net AWS data is necessary. We present a full reprocessing of the historical GC-Net AWS dataset with increased attention to the filtering of erroneous measurements, data correction, and derivation of additional variables: continuous surface height, instrument heights, surface

albedo, turbulent heat fluxes, 10 m ice and firn temperatures. This new augmented GC-Net Level 1 (L1) AWS dataset is now available at https://doi.org/10.22008/FK2/VVXGUT (Steffen et al. 2022) and will continue to be refined. The processing scripts, latest data and a data-user forum are available at https://github.com/GEUS-Glaciology-and-Climate/GC-Net-level-1-data-processing. In addition to the AWS data, a comprehensive compilation of valuable metadata is provided: maintenance reports, yearly pictures of the stations and the station positions through time. This unique dataset provides more than 320 station-years of high quality atmospheric data and is available following FAIR data and code practices.

1 Introduction

1.1 Background

The Greenland Ice Sheet plays a substantial role in the global climate system. As a low-temperature topographic obstacle, the ice sheet exerts important influences to regional atmospheric circulation (Bromwich et al., 1993, Hahn et al., 2020). Additionally, the majority of the ice sheet is covered with a highly reflective perennial snow cover and an overall negative net radiation budget, which makes the ice sheet a net cooling element in the global climate system (e.g. Toniazzo et al., 2004, Ridley et al., 2005). Recently, however, ice discharge via marine terminating outlet glaciers and seasonal melting of the ice sheet have both been increasing (e.g. IMBIE, 2020; Mankoff et al., 2021). This has increased the freshwater flux into the North Atlantic, impacting ecosystems (e.g. Oksman et al., 2022), influencing ocean circulation (e.g. He and Clark, 2022) and contributing to global sea-level rise (Nerem et al., 2018). In spite of the development of remote sensing techniques and weather modeling, the in-situ measurement of ice sheet surface climate variables remains paramount to improve our understanding of the Greenland Ice Sheet response to climate variability.

1.2 History of the Weather Stations on the Greenland Ice Sheet

The Greenland Climate Network (GC-Net) of Automated Weather Stations (AWS) adds to a long history of meteorological observation on the Greenland Ice Sheet. The study of the Greenland Ice Sheet's meteorology began with overland expeditions during the late 19th and early 20th centuries. After the second world war, purpose-built mechanized vehicles made it possible to transport the personnel and equipment required to maintain staffed stations on the ice sheet. The British North Greenland Expedition (BNG, 1952-1954) under the leadership of C.J.W. Simpson, traversed the ice sheet in North Greenland, establishing a temporary weather station at North Ice (Simpson, 1955). The contemporaneous French Expédition Glaciologique Internationale au Groenland (EGIG) was undertaken as a series of traverses between 1949 and 1967 under the leadership of Paul-Émile Victor (Finsterwalder, 1959). The larger EGIG effort included four staffed ice sheet stations: Camp IV, Camp VI, Station Centrale and Station Jarl-Joset/Dumont (Fristrup, 1962). Together, the BNG and EGIG expeditions provided some of the first reliable year-round meteorological records from the high-elevation ice sheet interior. U.S. military ice sheet sites also represent a valuable source of meteorological data (Menne et al., 2012; Jensen, 2022). These

include weather stations associated with the Distant Early Warning stations DYE-2 and DYE-3 (1959-1988) and Camp Century (1960-1964).

Since the 1980's, the ice sheet summit has been a focus of automated meteorological observations. In 1987, the University of Wisconsin-Madison installed a network of eight AWS around the ice sheet summit (Stearns and Weidner, 1991; Weidner and Stearns, 1991; Shuman et al., 2001). These stations supported both the Greenland Ice Sheet Project II (GISP2) and Greenland Ice Core Project (GRIP), two contemporaneous deep ice-core drilling projects. One of these stations captured the coldest temperature ever recorded in the northern hemisphere (-69.6 °C) in December 1991 (Weidner et al., 2020). This weather station network lasted until 1998. From 1991 to 1994, the Danish Meteorological Institute (DMI) operated an AWS at the GRIP-summit site. This station was moved 33 km to the GISP2 site, now known since 1997 as Summit. This DMI Summit AWS was decommissioned on 12 August 2020. DMI also operated an AWS from 1987 to 1988 on the Renland ice cap, East Greenland. The U.S. National Oceanic and Atmospheric Administration (NOAA) has also operated an independent AWS at Summit Station since 1997.

Numerous other institutions have also maintained ice sheet AWS for limited times and locations since the 1990s (e.g. Heinemann, 1999; Kendrick et al. 2018; Samimi et al., 2021; Covi et al. 2022, MacFerrin et al., 2022). Although multi-decade time-series are needed to resolve climatic trends, these short-lived AWS remain valuable to understand meteorological processes.

The Institute for Marine and Atmospheric research Utrecht (IMAU) of Utrecht University has overseen a sustained surface climate monitoring effort since 1990. Four ice sheet AWS were established upstream from the Russell Glacier near Kangerlussuaq, West Greenland (Oerlemans and Vugts 1993; van den Broeke et al., 1994; van de Wal and Russell 1994). These ice sheet AWS, designated S4, S5, S6, S9, ranged from the low ablation area at approximately 300 m above sea level (a.s.l.) to the equilibrium line at 1520 m a.s.l. A fifth AWS (S10) was installed in the lower accumulation area at 1850 m a.s.l. between 2010 and 2016. These AWS, as well as an East Greenland site in the firn aquifer region (Reijmer et al., 2019), continue to operate today.

The Meteorological Research Institute (MRI) at the Japan Meteorological Agency, in collaboration with Hokkaido University and the National Institute for Polar Research, began installing ice sheet AWS in Northwest Greenland in 2012 (Aoki et al., 2014; Matoba et al. 2015; Nishimura et al., 2023). Over the following years, the MRI installed and maintained the SIGMA-A and SIGMA-D AWS respectively at 1490 and 2100 m a.s.l. on the ice sheet, as well as the SIGMA-B AWS on the Qaanaaq ice cap at 944 m a.s.l.

The Geological Survey of Denmark and Greenland (GEUS), which was formed in 1995 from the Geological Survey of Greenland (GGU) and the Danish Geological Survey (DGU), has made on-ice glaciological and meteorological observations in Greenland since 1978. The first fully automated climate station operated between 1979-1983 near the margin of Qamanarssup Sermia (Olesen and Braithwaite, 1989). That effort was followed by other on-ice stations at Amitsuloq Ice Cap (1981-1990), and then Isortuarsuup Tasia and Paakitsup Akuliarusersua (both 1984-1987) and Storstrømmen Glacier (1989-1994; Olesen and Andreasen, 1983; Olesen and Braithwaite, 1989). In the 1990s, AWS were operated on

Nioghalvfjerdsfjorden Glacier (1996-1997), Imersuaq (1999–2002), Hans Tausen Ice Cap (1994-1995), and Mittivakkat Glacier (1995-present; Thomsen et al., 1999; Reeh et al., 1999; Reeh et al.. 2001; Braithwaite et al., 1998; Konzelmann and
105 Braithwaite, 1995). In the 2000s, newer station designs were introduced and operated around Greenland (van As et al., 2009). These sites include: Narsap Sermia (2003-2006) close to Nuuk; Sermersuaq, a.k.a. Steenstrup Glacier, (2004-2008) along the Melville Bay coast (van As, 2011); Helheim Glacier in Southeast Greenland (2008-2010, Andersen et al., 2010), and Arcturus Gletscher at Malmbjerg, East Greenland (2008-2010, Citterio et al. 2009). Since 2007, GEUS has operated on-ice AWS via the Programme for Monitoring the Greenland Ice Sheet (PROMICE; http://www.promice.org), in collaboration with the
110 Technical University of Denmark (DTU) and Asiaq Greenland Survey. Between 2008 and 2010, 23 PROMICE AWS were installed in the ice sheet ablation area, with one station in the ice sheet accumulation area (Ahlstrøm et al., 2008; Fausto et al., 2021). GEUS is also involved in the GlacioBasis project, as part of the Greenland Ecosystem Monitoring (GEM) programme (https://g-e-m.dk). The GlacioBasis project has been monitoring glacier surface mass balance at the A.P. Olsen Ice Cap in East Greenland with three on-ice AWS operational since 2008 and on the Chamberlin Glacier on Disko Island, West Greenland,
115 with two AWS operating since 2015.

1.3 The Greenland Climate Network (GC-Net)

In 1990, ETH Zürich, in collaboration with GGU/GEUS, established an on-ice research camp with a meteorological tower in West Greenland, ~89 km east of Ilulissat, near the ice sheet equilibrium line (Ohmura, 1991, 1992; Greuell and Konzelmann 1994). In 1992, Konrad Steffen initiated continuous meteorology observations at this site which became
120 informally referred to as "Swiss Camp" (Steffen, 1995). In 1995, this research station became the starting point of GC-Net which expanded to include accumulation-area AWS distributed across the ice sheet. Under the NASA Program for Arctic Regional Climate Assessment (PARCA), which sought to provide the first assessment of Greenland Ice Sheet mass balance (Thomas, 2001), a network of 18 AWS were deployed with support from the U.S. National Science Foundation (NSF) (Steffen et al., 1996, Steffen and Box, 2001). Additional GC-Net sites were later added and some sites were discontinued due to
125 logistical constraints and environmental challenges.

Through the project's timespan, GC-Net accumulated 31 AWS at 30 Greenland sites (Table 1, Figure 1A). The majority of the GC-Net sites were located in the ice sheet accumulation area (17 AWS), while 11 stations operated in the ablation area. The only AWS at the equilibrium line altitude (ELA) were the two AWS at Swiss Camp and Petermann ELA, although they shifted into an ablation regime in recent decades (e.g. McGrath et al., 2013). There are 16 AWS at 15 sites with
130 more than 15 years of data, 6 stations with 5-15 years of measurements, and 12 AWS that have been active less than 5 years (Table 1). The majority of the GC-Net AWS have a two-level design (Figure 1B) and six AWS are single-level "smart stake" AWS (Figure 1C), as described in Albert (2007). At Swiss Camp, meteorological observations are available for over 32 years. 16 AWS were still active in 2020 when the first AWS were decommissioned and replaced by modern AWS. All these data are contained in the GC-Net Level 1 dataset described here. The typical meteorological variables measured by the GC-Net stations
135 are: air temperature (TA), relative humidity (RH), wind speed (SW) and direction (DW), air pressure (P), downward and

reflected shortwave radiation fluxes (ISWR and OSWR), net radiation flux (NR), surface height (HS) and snow, firn or ice temperatures at 10 levels (typically each meter) below the surface (TS) (Figure 1B). We also include in this dataset three AWS of similar design as the GC-Net stations installed by K. Steffen's team on the Larsen C Ice Shelf, Antarctica and which went through the same re-processing as the GC-Net AWS data (Kuipers Munneke et al., 2017; McGrath et al., 2021).

140   In 2020, after delivering nearly thirty years of GC-Net service, Konrad Steffen died in an accident during fieldwork at Swiss Camp. His scientific contributions to the ice sheet research community have been highlighted by Box et al. (2021). Following Steffen's tragic death, and according to a plan already initiated with him, GEUS took over the climate monitoring at the main GC-Net sites. GEUS began maintaining and replacing individual stations in 2021, while the Swiss Federal Institute for Forest, Snow and Landscape Research (WSL) compiled the satellite transmissions until they stopped in 2022. By 2022,

145   the majority of the original GC-Net stations have been replaced, with the exception of the Summit and Petermann ELA AWS, which are planned to be replaced in the coming years. These new GEUS-maintained AWS, which will carry forward the name of "GC-Net", will be described in a separate publication and their data are distributed through https://promice.dk (GEUS, 2020; How et al., 2022a). Developing the historical GC-Net data into a quality-controlled, well-documented, open-access, FAIR product (Findable, Accessible, Interoperable and Reusable, Wilkinson et al., 2016), operating seamlessly with the

150   contemporary GEUS-era GC-Net data, is the primary motivation of the work presented here.
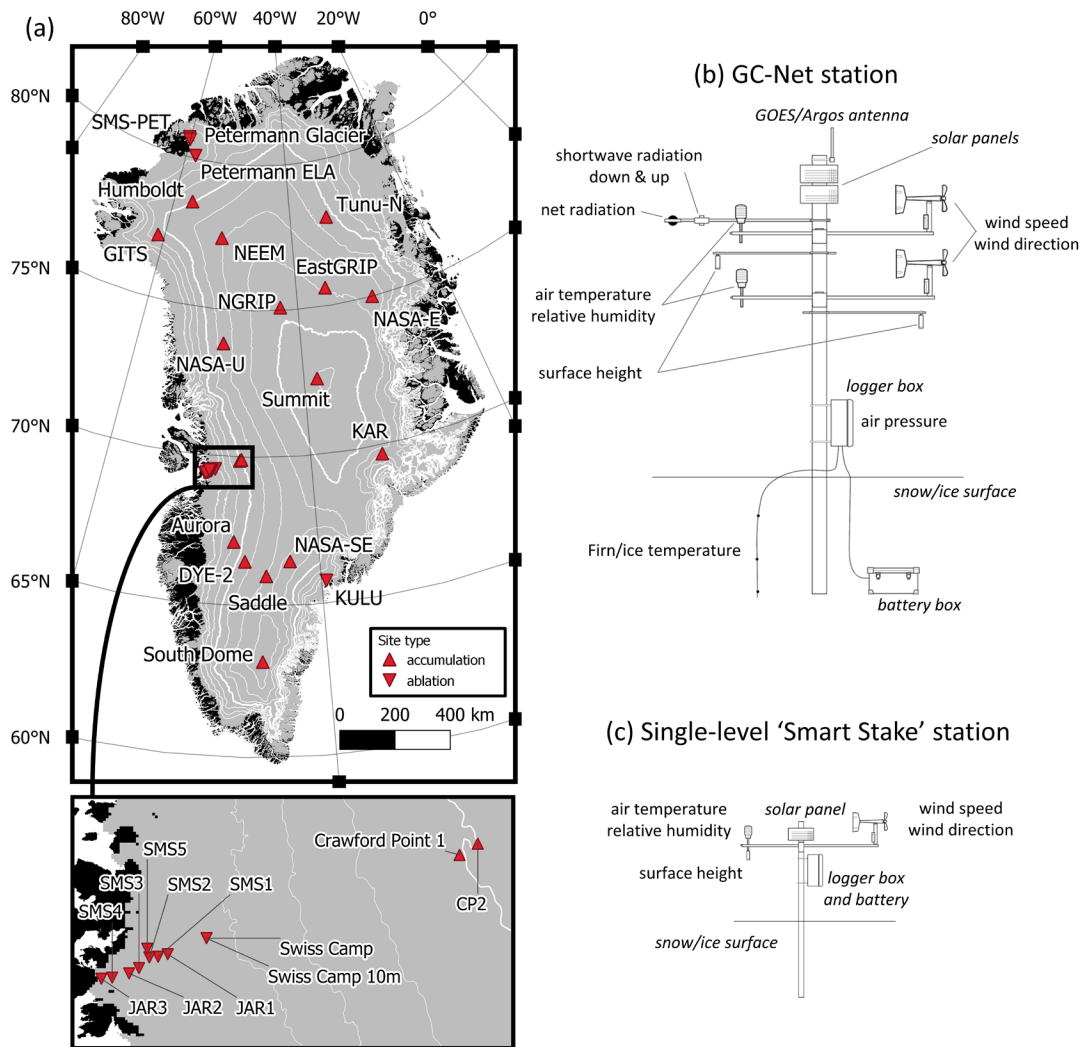
Figure 1. (a) GC-Net weather stations in Greenland. Thick white lines are 2000 and 3000 m elevation contours while thin white lines are 250 m elevation contours. (b) Design of the GC-Net weather station (two-level design). (c) Design of the single-level 'Smart Stake' station.

Table 1. List of the GC-Net AWS with coordinates (in the WGS84 reference system) and date of installation/decommission. The coordinates are the long-term average location or best available values. When possible, temporally resolved coordinates are also provided in the metadata.

Name	Latitude (°N)	Longitude (°E)	Elevation (m)	Date of installation	Last valid time	Length of record (years)	Type
Swiss Camp 10m	69.5556	-49.3647	1138	1990-05-09	2020-11-03	30.51	ablation
Swiss Camp	69.5556	-49.3647	1138	1995-01-01	2022-08-03	27.61	ablation
Crawford Point 1	69.8742	-47.0242	2022	1995-05-23	2020-07-22	25.18	accumulation
NASA-U	73.8407	-49.5265	2369	1995-05-31	2023-06-18	28.07	accumulation
GITS	77.1378	-61.0411	1887	1995-06-07	2021-08-13	26.20	accumulation
Humboldt	78.5283	-56.8423	1950	1995-06-22	2023-06-30	28.04	accumulation
Summit	72.5797	-38.5045	3254	1996-05-13	2022-09-20	26.37	accumulation
Tunu-N	78.0188	-33.9668	2113	1996-05-16	2023-06-20	27.11	accumulation
DYE-2	66.4820	-46.2908	2165	1996-05-24	2023-06-14	27.07	accumulation
JAR1	69.4933	-49.7142	900	1996-06-19	2019-09-08	23.24	ablation
Saddle	65.9999	-44.5026	2451	1997-04-20	2021-10-16	24.51	accumulation
South Dome	63.1489	-44.8175	2878	1997-04-23	2021-06-21	24.18	accumulation
NASA-E	75.0023	-29.9838	2610	1997-05-03	2022-09-20	25.40	accumulation
CP2	69.9133	-46.8547	1990	1997-05-12	2001-05-29	4.05	accumulation
NGRIP	75.0998	-42.3326	2950	1997-07-09	2010-05-08	12.84	accumulation
NASA-SE	66.4779	-42.4951	2360	1998-04-24	2019-09-26	21.44	accumulation
KAR	69.6994	-33.0006	2579	1999-05-19	2001-06-07	2.05	accumulation
JAR2	69.4200	-50.0575	568	1999-05-30	2013-06-16	14.06	ablation
KULU	65.7585	-39.6018	878	1999-06-17	2000-09-14	1.25	ablation
JAR3	69.3944	-50.3100	323	2000-05-28	2004-05-25	3.99	ablation
Aurora	67.1358	-47.2922	1798	2000-06-24	2001-05-06	0.87	accumulation
Petermann Glacier	80.6836	-60.2931	~70	2002-06-04	2006-05-01	3.91	ablation
Petermann ELA	80.0993	-58.1497	907	2003-05-23	2022-09-20	19.34	ablation
NEEM	77.4413	-51.0999	2460	2006-03-29	2022-09-20	16.49	accumulation
EastGRIP	75.6268	-35.9801	2653	2014-05-17	2023-06-22	9.10	accumulation
SMS1*	69.4822	-49.8017	822	2001-01-01	2006-05-01	5.33	ablation
SMS2*	69.4778	-49.8828	727	2001-01-01	2006-05-01	5.33	ablation
SMS3*	69.4403	-49.9703	605	2001-01-01	2006-05-01	5.33	ablation
SMS4*	69.4013	-50.2108	387	2001-01-01	2003-05-01	2.33	ablation
SMS5*	69.5056	-49.9093	~762	2001-01-01	2003-05-27	2.40	ablation
SMS-PET*	80.6033	-60.0536	~50	2002-06-01	2004-05-15	1.96	ablation
LAR1	-68.1411	-63.9519	~50	2008-12-23	2012-12-25	4.01	Antarctic ice shelf
LAR2	-67.5764	-63.2575	~50	2008-12-22	2011-11-15	2.90	Antarctic ice shelf
LAR3	-67.0317	-62.6503	~50	2009-08-10	2011-11-08	2.25	Antarctic ice shelf

160 * Single-level "smart stake" AWS

2. Network Description

The GC-Net sites were partly chosen in synergy with existing science projects or existing logistic links. The GC-Net program was formally initiated in 1995, with the installation of Swiss Camp, Crawford Point 1, NASA-U, GITS and Humboldt AWS. The Swiss Camp 10 m meteorological tower had been operating since 1990, continuously since June 1991 (Ohmura et

165 al., 1991, 1992). The NASA-U, GITS, and Humboldt stations were established in tandem with c. 500 m deep ice coring studies

sponsored by NSF and NASA (Bales et al., 2001a, 2001b; Mosley-Thompson et al., 2001, 2005). GITS (Greenland Ice Training Site) is located c. 5.5 km southeast of the Camp Century military base and ice core location, which, at the time, served as a practice 'skiway' for the US 109th Air National Guard ski-equipped LC-130H. The Crawford Point 1 station was installed upstream of Swiss Camp to represent the percolation area, extend the altitudinal profile to 2000 m, and to connect that with the Summit AWS record (McGrath et al., 2013). The precise location of Crawford Point (selected by John Crawford, Jet Propulsion Laboratory, California Institute of Technology) is the place where both ascending and descending NASA satellite orbits of interest intersected the 2000 m elevation contour. This contour was the focus of an early PARCA mass balance perimeter (Thomas et al., 2000).

In 1996, four AWS were installed. The Tunu-N AWS was installed in tandem with PARCA-sponsored coring where ice sheet snow accumulation exhibits a large-scale minimum (Sigl et al., 2015). The DYE-2 AWS was installed at the former military station of the same name. DYE-2 carries forward a legacy of glaciology and climatology measurements associated with the initial construction of the military station in 1959. DYE-2, later known as Camp Raven, now serves as the practice 'skiway' for the US 109th Air National Guard and is home for many other measurements (e.g. Samimi et al., 2020; MacFerrin et al., 2022). The JAR1 AWS was installed in the ablation area down-glacier from Swiss Camp. The Summit AWS was installed c. 1.4 km west of the GISP2 ice core that had been completed in 1993.

In 1997, South Dome, Saddle and NASA-E stations were installed alongside NASA-sponsored shallow ice-coring (Mosley-Thompson et al., 2001) and firn densification work (Hamilton and Whillans, 2000). The South Dome station is situated at the highest point on the ice sheet's South Dome, while Saddle station is situated at the lowest point on the main ice sheet topographic divide between Summit and South Dome. The same year, the CP2 station was installed ~8 km northeast from the Crawford Point AWS to capture surface topographic undulation-scale accumulation and climate variability. In 1997, the NGRIP AWS was installed at the site of a deep ice core drilling site (Dahl-Jensen et al., 2002). NGRIP AWS was discontinued in 2010 when the drilling was completed.

In 1998, NASA-SE was the last PARCA site where an AWS was installed in tandem with firn coring. In 1999, the Kangerdlugssuaq Accumulation Region (KAR) AWS was installed and the KULU AWS was installed within reach from Kulusuk airport in East Greenland. The same year, the JAR transect in the ablation area west of Swiss Camp received its second station JAR2. The KULU and KAR stations were both discontinued in 2000 and 2001 due to the challenges that represented strong winds, high snow accumulation and remoteness of East Greenland for station maintenance.

In 2000, the Aurora AWS was installed on the ice sheet ~150 km east of Kangerlussuaq in western Greenland in connection to an on-ice automobile test track. The AWS was discontinued in 2001 when the car testing project stopped. Also in 2000, the JAR transect received its third and lowest station JAR3. In 2002, Petermann Glacier AWS was installed on the floating tongue of Petermann Glacier in northwest Greenland and the Petermann ELA AWS was installed in the following year. These two AWS provided surface climate data needed for the study of the ice-ocean interaction at Petermann Glacier (Rignot and Steffen, 2008). The Petermann station was discontinued due to the presence of crevasses. Crevasses and low snow accumulation are also now challenging aircraft access to Petermann ELA. In 2006, the NEEM AWS was installed in

preparation of the North Greenland Eemian Ice Drilling project (NEEM, 2013). The NEEM AWS remained at that location after the drilling project finished and a new AWS was installed at EastGRIP in 2014 when a new deep drilling project started.

In 2001, five single-level 'smart stakes' AWS (Figure 1C) were installed in the lower ablation area of Sermeq Avannarleq glacier (Albert, 2007), neighbour of Sermeq Kujalleq (Jakobshavn isbræ). These smart stakes were serviced by snowmobile from Swiss Camp until 2003 (SMS4-5) and 2006 (SMS1-3). JAR3 was discontinued in 2004 due to the upstream expansion of crevasses and JAR2 was discontinued in 2013 for similar reasons.

Three AWS were installed on the Larsen C ice shelf, Antarctica, in 2008 (Kuipers Munneke et al., 2017; McGrath et al., 2021). Given the similarities in the station design and data structure, we include these three Larsen C stations in this curated Level 1 (L1) data product version of otherwise Greenland-focused GC-Net data.

Beginning in August 2020, GEUS began maintaining the GC-Net stations at Swiss Camp and JAR1. In 2021, GEUS installed its replacement AWS at Crawford Point 1, NASA-SE, South Dome, GITS, Saddle, NASA-U, NEEM and DYE-2. Existing stations were removed from the first four sites, DYE-2 was raised and serviced, and the remaining historical stations were left as they were. In 2022, DYE-2, Saddle, Humboldt, NEEM, NASA-E and Tunu-N, were visited but no maintenance was carried out apart from downloading data from the logger and raising the lower boom arm at NASA-E. Also in 2022, GEUS installed new AWS at Humboldt, NEEM, NASA-E and Tunu-N next to the original AWS. In 2023, GEUS decommissioned DYE-2, NASA-U, EastGRIP, Humboldt, Tunu-N. In the coming years, GEUS plans to visit Petermann ELA, NEEM, NASA-E, Swiss Camp and Summit, retrieve their data and decommission the historical AWS.

3 Station description

3.1 Station design and maintenance

The main characteristic of the GC-Net AWS is its two levels of measurements for air temperature, relative humidity, wind speed and direction. In the L1 dataset, the variables labeled with "1" (e.g. TA1) were measured or derived from the lower level. The variables labeled with "2" (e.g. TA2) were measured or derived from the upper level. The two levels are typically placed with 1.2 m vertical separation, although other spacing was used on occasions when the station could not be raised, and the lower level was at risk of getting buried by accumulating snow.

The most common GC-Net masts were aluminium tubes with 4" (10.16 cm) outside diameter, initially 6.4 m in length. Ablation area sites (JAR2-3, PET ELA, PET Glacier and the SMS) used a 3" (7.62 cm) mast. Both the 4" and 3" outside diameter mast tubes had 0.25" (0.635 cm) wall thickness. The masts were inserted into a c. 3.2 m deep hole from a borehole taken in firn using a core drill, or in ice using a steam or mechanical drill. The JAR1 station was the only ablation area station with the 4" (10.16 cm) outside diameter mast. The masts were raised (accumulation sites) or lowered (ablation sites) using a 6 m high tripod and winch system (Figure 2); separating the upper section of the mast, inserting an extension in the case of accumulation area sites (or removing a section at ablation sites), then lowering the upper section back down onto the base mast section. Over time, the base pipe reached a length of up to 30 m at NASA-SE. Low accumulation sites (e.g. Tunu-N, Humboldt,

NASA-E) could be visited every one or two years. High accumulation sites, in particular NASA-SE and South Dome, needed annual visits to prevent burial by accumulating snow. Ablation area sites also needed frequent visits to prevent the mast from melting out and the AWS from collapsing. It was not uncommon to find ablation area AWS masts leaning. Because of the
235 initial (1995- ca. 2000) use of guy wires, differential compaction or the failure of one wire led to station tilt. When the station tilt was too critical, the mast was re-drilled (e.g. at DYE-2 in 2019 and 2021).

For information on the design of the meteorological tower and pre-1995 AWS at Swiss Camp, more details can be found in Ohmura et al. (1991, 1992) and Steffen et al. (1995, 1996).

240 **Figure 2. Raising the Crawford Point 1 mast, 3 May 2005. K. Steffen (left), R. Huff (right). Photo J. Box.**

3.2 Instrumentation

The standard instrumentation of the GC-Net AWS is provided in Table 2, compiled from Steffen et al. (1996), Steffen and Box (2001), Box and Steffen (2001a), Steffen et al., (2003, 2005, 2006). The primary air temperature measurement was done by a Type-E thermocouple (variables TA1 and TA2 in the L1 dataset). Secondary air temperature readings were done by
245 CS500 thermometers (variable TA3 for the lower level and TA4 for the upper level in the L1 dataset) but these sensors did not accurately measure temperatures below -40°C. While efforts were made to keep the instrumentation consistent, exceptions include shifting the thermohygrometer from Vaisala INTERCAP 50YC (a.k.a. HUMICAP 180 packaged by Campbell Sci. as CS500) to the Vaisala HMP45 after ca. 1999, and from ca. 2008, switching to the Vaisala HMP155. The Swiss Camp AWS had less consistent air temperature and hygrometer instrumentation, as the site was used to test emerging technologies,

including tests of fan-aspirated temperature shields. Barometers were initially a Vaisala PTB101A, replaced in c. 1999 with a PTB101B. The LI-COR LI-190SZ instrument measuring downward and reflected shortwave radiation and surface albedo, is sensitive to the 0.4-0.7 µm spectral range. The REBS Q7.1 net radiation sensor is sensitive to the 0.25 - 60 µm spectral range. A domeless version 1 Kipp & Zonen NR-Lite net radiometer with spectral range of 0.2-100 µm was used at Summit and Swiss Camp starting in ca. 2000. See Brotzge and Duchon (2000) for an intercomparison of the different radiometers. The snow, firn and ice temperatures were measured by 10 type-T thermocouples inserted in the snow/firn/ice with a 1 m spacing ranging from 1 to 10 m depth (Sampson, 2009). Most of these temperature strings were discontinued in 2010. The single-level Smart Stake AWS (Table 1) were not equipped with temperature strings. The surface height was measured with two SR50 sonic rangers. In the L1 dataset, these measurements are corrected for the effect of air temperature on the speed of sound according to the SR50 user manual (Campbell Scientific, 2007na).

From 1995 to around 2000, the data logger was a Campbell Scientific CR10. These were replaced starting in 1999 with a CR10x until 2009 when CR1000 loggers were progressively introduced. The original Swiss Camp data loggers were CR21, then CR21x running the 10 m tower until ca. 1998.

Table 2. Instrumentation overview.

Parameter	Variable name	Instrument	Accuracy	Sample interval
Air temperature 1	TA1, TA2	Type-E thermocouple	0.1 °C	60 s
Air temperature 2	TA3, TA4	Vaisala 50YC within a Campbell Scientific CS500	0.1 °C	15 s
Relative Humidity	RH1, RH2	Vaisala INTERCAP 50YC Vaisala HUMICAP HMP45 or HMP155	5% < 90%, 10% > 90%	60 s
Wind speed	VW1, VW2	RM Young propeller-type Vane	0.1 m s^{-1}	60 s*, 15 s
Wind direction	DW1, DW2	RM Young propeller-type Vane	5°	60 s
Air pressure	P	Vaisala PTB101B	0.1 hPa	60 min
Surface height change	HS1, HS2	Campbell Scientific SR50	1 mm	10 min
Shortwave radiation Albedo	ISWR, OSWR Alb	Li Core LI-190 or 200SZ	5-15%	15 s
Net radiation	NR	Campbell Scientific REBS Q7.1 Kipp & Zonen NR Lite2**	5-50%	15 s
Longwave radiation**	ILWR, Tsurf	Kipp & Zonen CG4 Eppley Pyrgeometer	4-7%	1-15 s
Snow/firn/ice temperature	TS1 … TS10	Type-T thermocouple	0.1 °C	15 s

Multiplexer	Campbell Scientific Am25T		
GPS time	Garmin	1 s	1 day
Solar panel	Campbell Scientific 10W or 20 W		

* sampling was changed from 60 to 15 s after 1999 for all sites except NGRIP.

** introduced at Swiss Camp and Summit in c. 2000.

Two data collection systems were used to transmit the GC-Net AWS data in near real-time. For sites south of 72°N, the National Oceanic and Atmospheric Administration (NOAA) Geostationary Operational Environmental Satellites (GOES) system was used. For sites north of 72°N, the Argos polar orbiting satellite system was used. K. Steffen found that the directional antenna for the more affordable GOES transmission worked at the higher latitude NEEM and EastGRIP sites. These transmissions allowed near-real time dissemination of the AWS data during the operation of the network. In the present dataset, data files retrieved from the loggers during site visits are used, unless only transmitted data are available.

For the instrumentation of the meteorological tower and pre-1995 AWS at Swiss Camp, more details can be found in Ohmura et al. (1991, 1992) and Steffen et al. (1995, 1996).

4 Data processing and enhancement

The GC-Net data has been processed with various software since its creation. From 1995 to 2004, GC-Net data concatenation of field-gathered or GOES/Argos transmissions was achieved using FORTRAN77 codes, followed by Interactive Data Language (IDL) scripts for application of calibration constants and the filtering of outliers (Box and Steffen, 2001b). The GC-Net data processing was then migrated in 2004 to Matlab scripts (Bayou and Steffen, 2011) where the user could exclude outliers via a graphical user interface. These two approaches lacked transparency and repeatability, and were conducted using commercial software. For the GEUS-led reprocessing, processing scripts are written in Python and in an open-source approach, allowing more transparency and straightforward repeatability via Git versioning (Vandecrux et al., 2023a). This re-processing could be done directly from the CR1000 logger files starting in 2009. For data collected by older loggers, the incomplete information about file headers and logger programs made it more complicated to work with these raw logger files. We therefore currently use historical files processed by J. Box from 1995 to 2005 and N. Bayou and K. Steffen from 2005 to 2009 as input for our work. For the Swiss Camp 10 m meteorological tower, both logger files and historical FORTRAN processing scripts were available, so we could re-process the raw logger files and apply the same calibrations as in the historical FORTRAN programs. The key steps of our transparent and open-source re-processing framework is detailed in the following paragraphs and in Figure 3.

The re-processing of the historical GC-Net data presented here follows the FAIR principles (Wilkinson et al., 2022) where i) both data, and crucial metadata, are *Findable* through this publication and through the referencing of the Dataverse on common web search platforms; ii) (meta)data are *Accessible* through an open and free data distribution platform; iii) the

data are *Interoperable* as the (meta)data are distributed in non-proprietary, machine-readable format; iv) the (meta)data are *Reusable* as the data are fully described and processed in a transparent way.

4.1 Data processing, filtering and adjustments

Ideally, the data processing should start from unaltered logger files (the "Level 0" dataset, L0), however, because the data loggers used before 2009 have changing file formats and no header, we currently use historical, processed and calibrated files (as produced for Box and Steffen, 2001a), until the time when CR1000 data loggers were introduced. To build the "Level 0 Merged" dataset (L0M, Figure 3), which is the starting point of our re-processing, we collect the available CR1000 logger files, apply the calibration coefficients to the radiation data and append them to the pre-CR1000, historical processed files. The data is then processed as illustrated in Figure 3. The first step is to remove periods where the sensor and/or station was not functioning, and no valuable information could be retrieved from the data. For each station, a CSV (comma-separated values) "flag" file lists these erroneous periods along with the sensor they apply to. The CSV flag file also contains for each flagged period a comment field explaining the reason for flagging, and the operator who applied the flag, can be indicated. The processing script reads this station-specific flag file and discards the listed variables for the given periods.
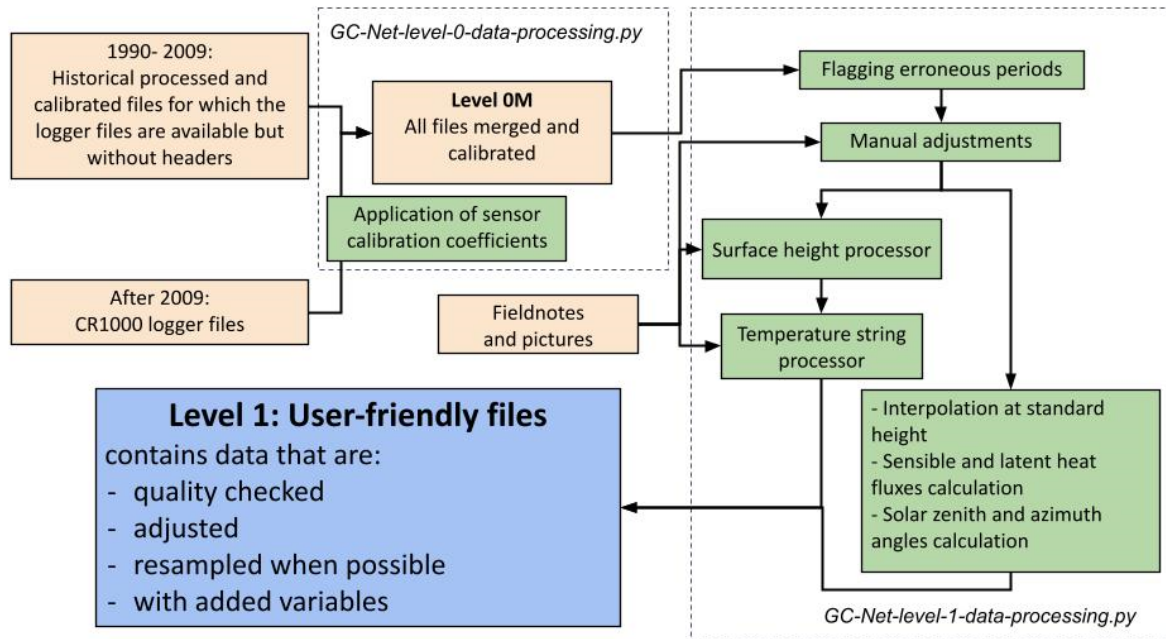
Figure 3. GC-Net data processing flow. Orange boxes indicate intermediate data products, green boxes indicate operations and the blue box is the final L1 data.

The next step adjusts the data for biases and filters noisy measurements. Filtering is done with another series of station-specific "adjustment" CSV files. Each adjustment file contains a list of time periods, variables, adjustment function name and adjustment parameters for a given station. The target variables can be passed as a list of space-separated variables

or as a regex (regular expression) string. The adjustment function names are self-explanatory (e.g. "add", "multiply", "rotate", "swap_with_", "min_filter, "max_filter"). The processing script then applies the given function on the listed variables during the specified period. These adjustments allow, for example, to correct for wind direction installed with an offset of 180°,

315 therefore giving rotated wind direction, adjust for a shift in air pressure due to a missing or changing offset in the barometer measurement, or for constructing the augmented or added variables listed in the next section (height of the wind sensors, continuous surface height). A comment for each modified period reports the motivation, e.g. a reported sensor malfunction, power failure, frozen anemometer propeller, or unlikely values after comparison with an external dataset. When the suspicious data and its adjustment were discussed online on the project's issue page (https://github.com/GEUS-Glaciology-and-

320 Climate/GC-Net-level-1-data-processing/issues), the URL to the discussion is given in the comment field of the flagging or adjustment file. Attention was given to harmonize all relative humidity into values relative to saturation water vapor pressure over water, so that they can be converted into values relative to saturation water vapor pressure over ice later in the processing script (see next section). All these adjustments were determined through the evaluation of station photos (Box et al., 2023), field notes (Vandecrux et al., 2023b), and comparisons with secondary AWS and regional climate outputs (Vandecrux, 2023).

325 Time shifts were applied to many stations to compensate for data logger clock drift. These time shifts were persistent at Humboldt where the logger clock was shifted by several months every year. The value of the time shift correction was chosen based on available field notes and on the comparison of the measured air pressure and temperature with values from the Regional Atmospheric Climate Model, RACMO (Noël et al., 2019).

Once the erroneous periods are removed and the adjustments applied, a last set of "standard" filters are applied: 1) a

330 set of standard minimum and maximum filters is defined in a "filter" CSV file, first giving limits for each variable at all or some stations (time specific min/max need to be listed in the adjustment CSV file); 2) a persistent value filter that detects periods where values do not change (e.g. anemometer covered in rime), 3) the removal of non-meaningful data such as wind direction in case of low (< 0.5 m s^{-1}) wind speed, or isolated surface height measurements. The report of the data treatment is compiled in a single file available here:

335 https://github.com/GEUS-Glaciology-and-Climate/GC-Net-level-1-data-processing/blob/main/out/report_with_toc.md.

The idea behind the open and transparent processing of the GC-Net data is that data users can investigate the site or variable of their interest, and see what type of filtering or adjustments have been applied. Data users can post issues on the processing repository with questions or pointing at sensor malfunctions not yet removed from the data. Thereby, this transparent interaction with the data from all users can benefit all users. This flagging and adjustment framework, developed

340 and tested on the GC-Net dataset is now also used for operational PROMICE AWS (https://github.com/GEUS-Glaciology-and-Climate/PROMICE-AWS-data-issues).

4.2 Augmented, corrected, and added variables

The GC-Net L1 dataset contains several variables that are derived or adjusted from the L0 data (e.g. instrument heights, relative humidity corrected for subfreezing conditions) and other variables that are added to the dataset to make the dataset easier to use (e.g. solar zenith and azimuth angles, time-stamped station position).

Instrument heights: Each station is equipped with two sonic rangers measuring the distance between each sensor and the surface (Table 2, Figure 1B). However, these sensors are not installed with a fixed height offset compared to the height-sensitive measurements (air temperature, relative humidity, wind speed and direction). Additionally, the offset between the sonic ranger and the other instruments changes for each station and can also change through time as the station is maintained. Consequently, the sonic ranger height from the L0 data are converted into instrument heights (HW1 and HW2) in the Level 1 dataset by a series of time specific adjustments to match the instrument height reported during station maintenance (Figure 4). The maintenance data, digitized from field books (Vandecrux et al., 2023b) are compiled in a spreadsheet also available in the metadata folder of the L1 dataset. For periods and sites where no measurements of sensor heights were reported, a photogrammetric estimation of instrument heights (Box et al., 2023a) was derived from available photos (Box et al., 2023b). In the L1 data, we made HW1 or HW2 match with the reported or estimated heights of the anemometer. On a leveled GC-Net AWS, the anemometer height should be the same as the TA/RH sensors. However, on many occasions, the tilt of the station (not recorded) led to obvious differences between the reported height of the TA/RH sensor and the reported HW (Figure 4). This error is currently not accounted for in the L1 product but can be investigated through evaluation of the field books, maintenance spreadsheet and the photo archive (Box et al., 2023b).
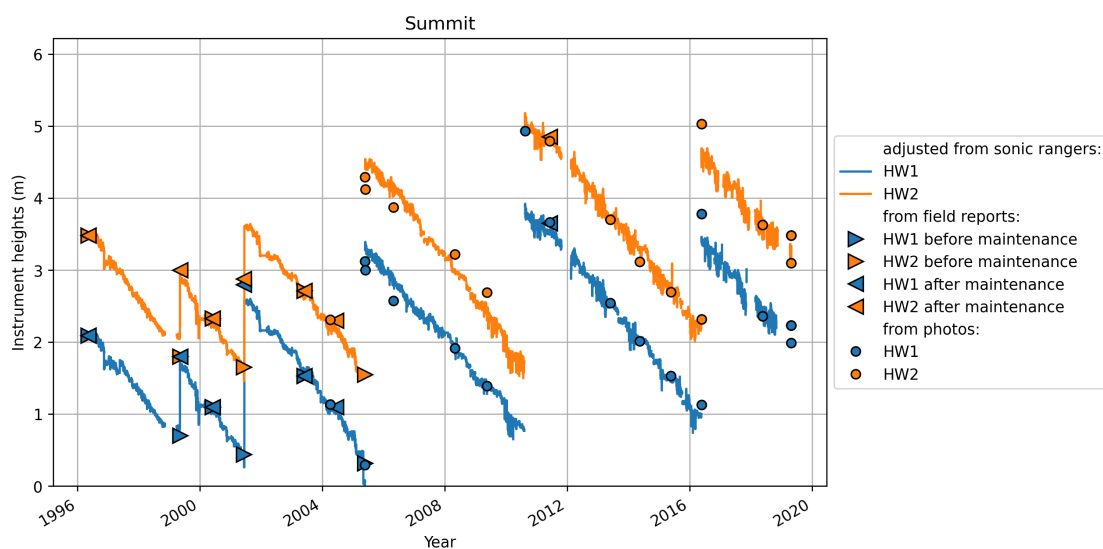
Figure 4. Instrument heights for the Summit AWS. Triangles are instrument heights measured by operators in the field (pointing right: before maintenance, pointing left: after maintenance) while the dots are heights estimated from field pictures.

Continuous surface height: The raw sonic ranger heights (HW1 and HW2 in the L0 dataset) and the height of the instruments
(HW1 and HW2 in the L1 dataset) include jumps whenever the station, or an instrument was shifted up or down. We reconstruct
a continuous surface height (HS1 and HS2 in the L1 dataset) by removing all these jumps in HW1 and HW2. The results at
different stations appear in Figures 4 and 5. The zero-height reference is arbitrarily set to the first recorded value. In cases
when the sonic rangers were failing, the height after the gap was adjusted so that the trend is preserved. Though, the assumption
of a purely linear trend means that data users should consider only the continuous periods for quantitative inferences.

Relative humidity correction and specific humidity calculation: The capacitance hygrometers used on the GC-Net stations
respond to relative humidity with respect to water. Thus, under sub-freezing conditions, Goff-Gratch equations (Goff and
Gratch 1946) are used to calculate the corrected relative humidity (RH1_cor and RH2_cor in the L1 dataset) with respect to
ice (Anderson, 1994, 1995). These corrected RH are then converted into specific humidity (Q1 and Q2 in the L1 dataset).
Relative correction and specific humidity calculation are done following the same scheme used for PROMICE AWS data
(Fausto et al., 2021) now available through the *pypromice* python package (How et al., 2022b).

Net radiation corrected from wind effect: The observations from both REBS Q7.1 and Kipp & Zonen NR-Lite instruments
are affected by the wind-driven, convective cooling of the instrument and are consequently corrected as specified by the
manufacturers (Campbell Scientific, 1996; Kipp & Zonen, n.d.). The corrected values are available under the NR_cor variable
in the L1 dataset.
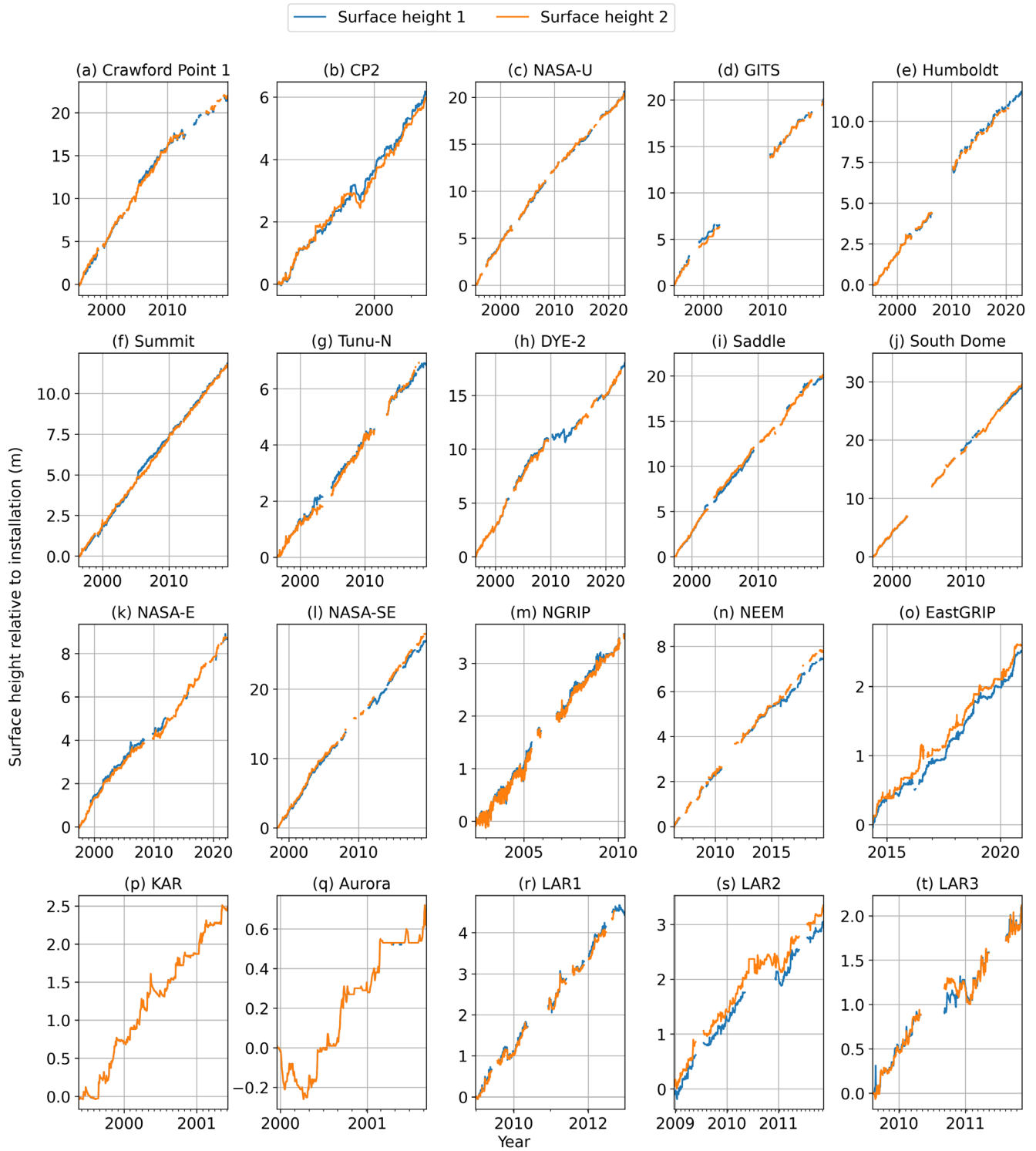
Figure 5. Overview of the reconstructed surface height for the GC-Net sites located in accumulation regions.
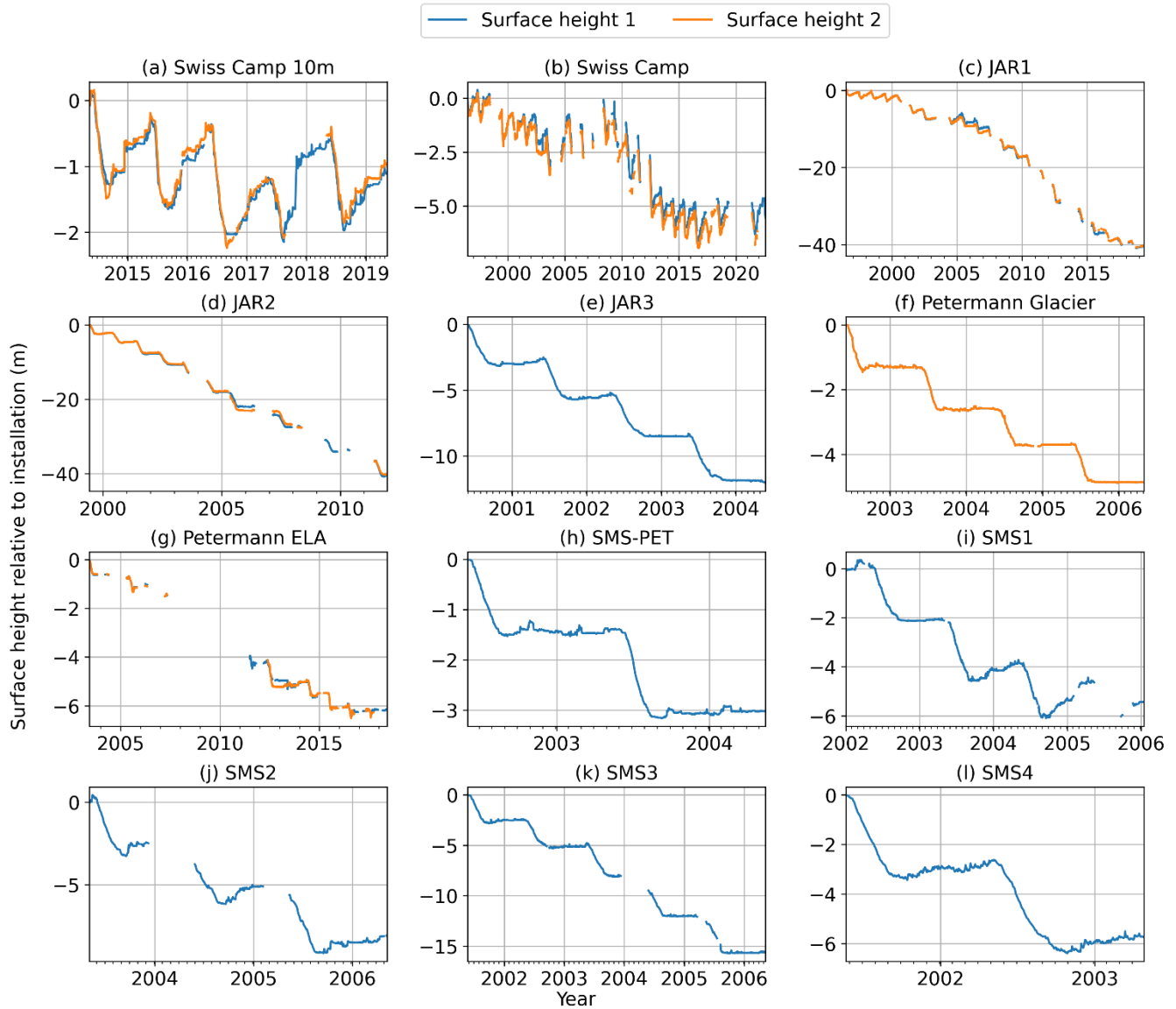
Figure 6. Same as Figure 5, but for ablation area sites.

385

Solar zenith and azimuth angles: The solar azimuth (SAA) and zenith angles (SZA) are key variables when using any in-situ irradiance measurement. We calculate, for each station location, SZA and SAA using the *pypromice* python package (How et al., 2022b).

Surface albedo: The surface albedo is calculated from hourly averages as the ratio of the reflected to downward shortwave irradiance. Hours with SZA > 70 °, low illumination conditions (ISWR or OSWR < 100 m W^{-2}) and impossible albedo values (<=0 or >=1) are discarded. The calculated albedo is very sensitive to instrument level and periods with frost obscuring one or both of the pyranometers. We therefore advise to use the more robust daily average albedo values, or a running hourly integration of daily values such as presented in van den Broeke et al. (2004); Stroeve et al (2013). We recommend caution when using the hourly albedo values until further assessment and correction of pyranometer sensor tilt is made. See Section 5.4 Dataset evaluation and known limitations for more detailed information.

Air temperature, relative humidity and wind speed at standardized height: In addition to the measurements at the two levels, the air temperature, relative humidity and wind speed are also provided at 2, 2, and 10 m (variables TA2m, RH2m, VW10m). For TA2m, RH2m, the inter/extrapolation is done linearly from the two measurement levels. For VW10m, we first extrapolate to 10 m using a logarithmic fit on the two measurement levels. If only one level is available or if the wind speed at the lower level is higher than at the upper level, the logarithmic fit cannot be used, we then estimate the 10 m wind speed using the upper-most available measurement and a theoretical logarithmic wind profile with a surface roughness length of 0.01 m (as used by K. Steffen in previous release of the GC-Net data).

Turbulent heat fluxes: The purpose of the two levels on the GC-Net AWS is to capture the near-surface gradients in TA, RH and VW, and to derive the turbulent sensible and latent heat fluxes resulting from these gradients (e.g., Box and Steffen, 2001; Cullen et al., 2014). The sensible and latent heat fluxes (SHF and LHF) are calculated using the method from Steffen and DeMaria (1996) as coded in the *JAWS* python package (Zender et al., 2018). SHF and LHF calculations are sensitive to data quality and accuracy of the instrument heights (Box and Steffen, 2001a) and should be used with caution.

Depth of the temperature strings and 10 m ice/firn temperature: The GC-Net AWS monitor snow, ice and firn temperatures through 10 thermocouples (Figure 1B). The depth of each sensor (DTS1-10 in the L1 dataset) is estimated for each time step from the available installation depth reported in field books and from the continuous surface height following a similar procedure as Vandecrux et al. (2020). Compaction of the firn between the sensors is not accounted for in the L1 dataset although Vandecrux et al. (2020) found that on the first year following the installation, firn compaction reduces the spacing by c. 15% near the surface and c. 3% down to 10 m depth. The ice or firn temperature at a standardized 10 m depth (TS_10m in the L1 dataset) below the surface is linearly inter- or extrapolated from the available measurements with the condition that at least one sensor is located within ± 1.5 m from the 10 m depth.

Station position through time: Over the three decades of measurements, the ice on which the GC-Net AWS are standing has been advected towards the ice sheet margin due to ice flow. We compiled all the available GPS measurements to document the AWS displacements (Vandecrux and Box, 2023c). For the stations located in areas of faster ice flow (Swiss Camp, Crawford Point 1, NASA-U, GITS, Tunu-N, DYE-2, JAR1, NASA-E, NASA-SE and Petermann-ELA) and when sufficient GPS measurements are available, we inter- or extrapolate the hourly position of the station by fitting a first order spline to the observed coordinates. These inter- or extrapolated coordinates are available in L1 data files as "Lat" and "Lon". The interpolation is done using a spline best fit and is therefore not exactly matching observations when available but rather looking

at the trend in sets of observed coordinates. This approach was more robust to inaccuracies in some of the handheld GPS positions. For the remaining stations (not moving or insufficient GPS measurements), the coordinates from Table 1 are included in the "Lat" and "Lon" variables in the L1 data files. An example of these measured and inter/extrapolated annual coordinates is given in Figure 7 for JAR1 AWS.
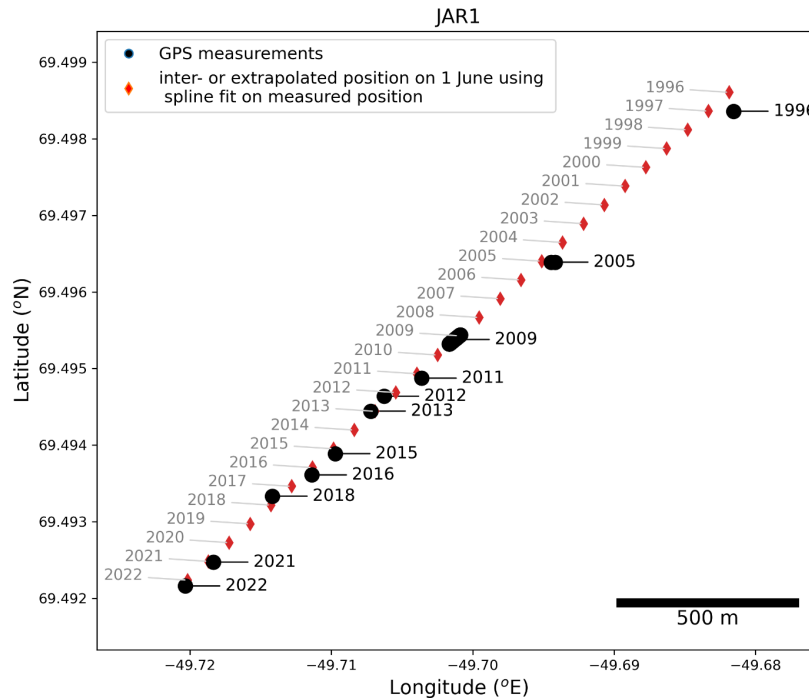
Figure 7. Example of handheld GPS observations of JAR1 AWS position (black dots) and interpolation to annual position using a spline fit of the observations (red diamonds).

5 Dataset overview

5.1 Format and structure

The GC-Net Level 1 dataset is made available in Non-binary Environmental Archive Date (NEAD) format, which is a CSV file with an added metadata header. The format is described in Iosifescu Enescu et al. (2020) and the pyNEAD python package (Mankoff and Vandecrux, 2023) is used to read and write NEAD files. The GC-Net Level 1 dataset contains both hourly and daily values in their respective folders, and, respecting the historical distribution of GC-Net data, the time stamp was set to the end of the measurement interval and documented accordingly in the NEAD file header. The data is divided into a folder for hourly averages and a folder for daily averages. A ReadMe text file, as well as CSV files listing the AWS reference coordinates and the variables contained in the L1 dataset are available in the dataset root directory. The compilations of

maintenance reports from the AWS are available at Vandecrux et al. (2023b), the field picture archive is stored at Box et al.

440   (2023b) and the collection observed GPS coordinates is available at Vandecrux et al. (2023c).
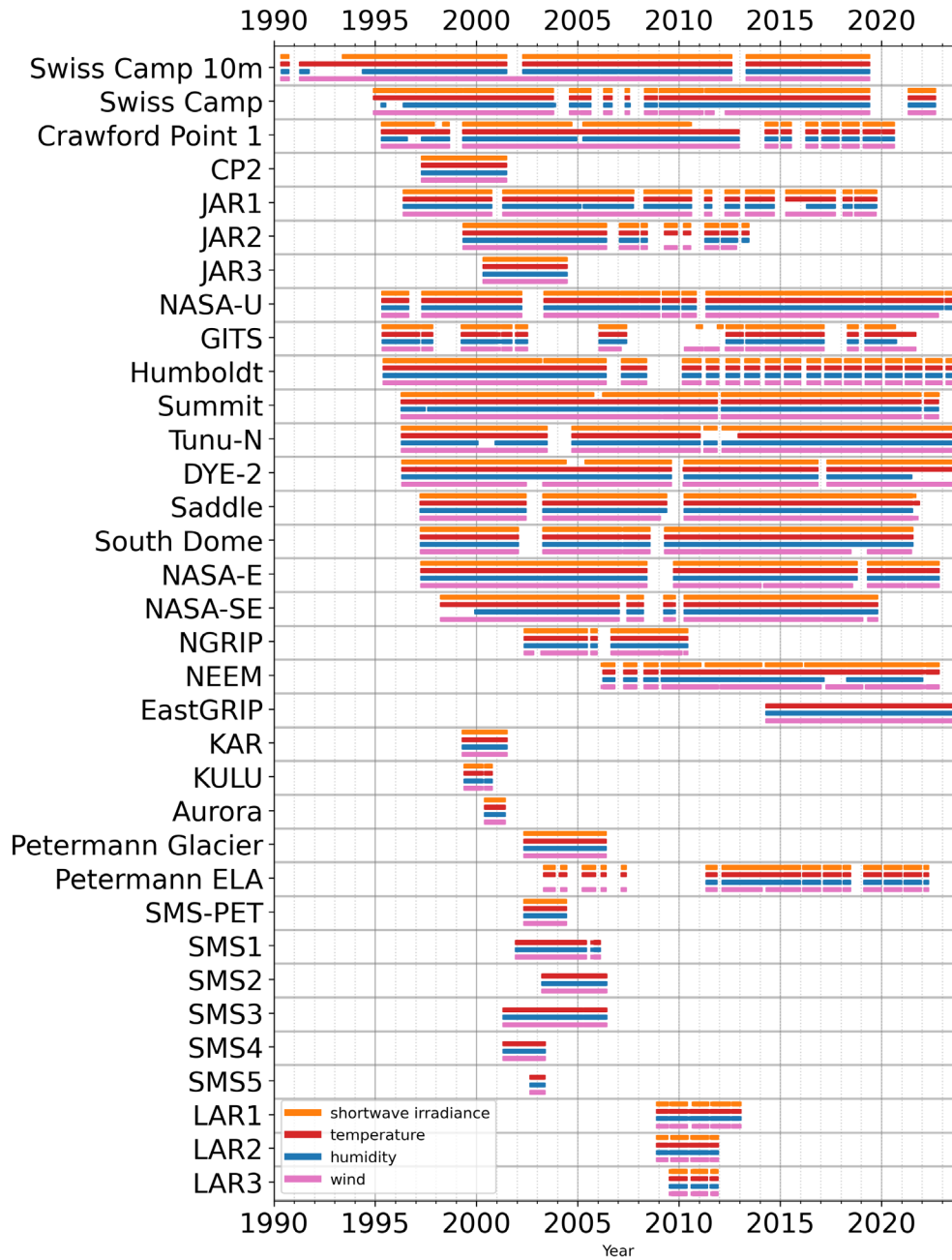
Figure 8. Data availability for shortwave irradiance, air temperature, humidity and wind speed/direction data.

5.2 Data coverage

445 Operating a weather station on the Greenland Ice Sheet is a technical and logistical challenge. The instrumentation, power management and data storage strategies were designed to withstand these harsh conditions. Yet many issues were reported through the years and these failures include among others: power shortage or short circuits (e.g. repeatedly at the GITS AWS), cables being pulled due to snow compaction, AWS getting buried when site visits were not made, AWS in the ablation area melting out and collapsing (mainly JAR1-3 and SWC AWS), logger clock malfunction (e.g. repeatedly at Humboldt), or

450 individual sensor failure due to extremely low temperatures, rime or liquid water. An overview of the data availability for the four main variables (shortwave irradiance, air temperature, humidity and wind speed/direction) is provided in Figure 8.

Table 3. Seasonal average near surface air temperature. The interpolated 2 m air temperature is used when the two levels are available, otherwise a single measurement level is used.

Site	Average near surface air temperature (°C)				
	Winter	Spring	Summer	Autumn	Year
Swiss Camp	-20.1	-14.4	-0.5	-12.2	-11.8
Crawford Point 1	-26.5	-20.2	-5.7	-19.4	-17.9
NASA-U	-33.0	-25.0	-8.9	-24.7	-22.9
GITS	-33.2	-25.8	-7.7	-23.6	-22.5
Humboldt	-36.5	-28.1	-8.4	-26.8	-24.9
Summit	-38.6	-30.8	-14.2	-31.1	-28.6
Tunu-N	-38.5	-29.9	-10.0	-29.8	-27.0
DYE-2	-27.2	-19.6	-5.4	-18.2	-17.6
JAR1	-18.0	-12.6	0.6	-10.4	-10.1
Saddle	-29.0	-21.2	-7.4	-20.8	-19.6
South Dome	-28.2	-20.5	-8.6	-19.8	-19.3
NASA-E	-38.0	-29.5	-12.2	-29.5	-27.3
NASA-SE	-28.8	-21.4	-8.0	-20.9	-19.8
Petermann ELA	-28.6	-20.7	-1.2	-18.2	-13.7
NEEM	-37.7	-29.4	-10.9	-29.4	-26.8
EastGRIP	-41.6	-30.6	-12.4	-30.5	-28.7

455 ## 5.3 Climatology at the GC-Net sites

The GC-Net weather stations are located primarily in the higher elevation accumulation zone of the ice sheet, with near-surface air temperature remaining below freezing year round (Figure 9) and annually increasing surface heights due to snow accumulation (compensated by the ice sheet motion, which is not measured by the AWS). The lowest average

temperatures are found at Summit station (Table 3), at the topographic high point of the ice sheet (3254 m a.s.l.). The Swiss
460   Camp, JAR and Petermann stations, which represent relatively higher temperatures at or below the ELA, are characterized by
above-freezing summer air temperatures (Table 3) and net annual ablation (loss in surface height).

All sites exhibit a distinct summer season between day of year 100-300, characterized by a peak in near-surface air
temperature during the warmest month of July (Figure 9). When compared to the winter season, the summer season shows
lower variability in near-surface air temperature and relatively low wind speeds (Figure 9 and 10). The winter season is
465   characterized by a prolonged period of consistently lower temperatures and higher winds spanning December through February
(Figure 9 and 10).

Many GC-Net stations are approaching a climatologically significant period of record (~30 years), providing valuable
records of long-term trends in both air temperature and surface-height change.
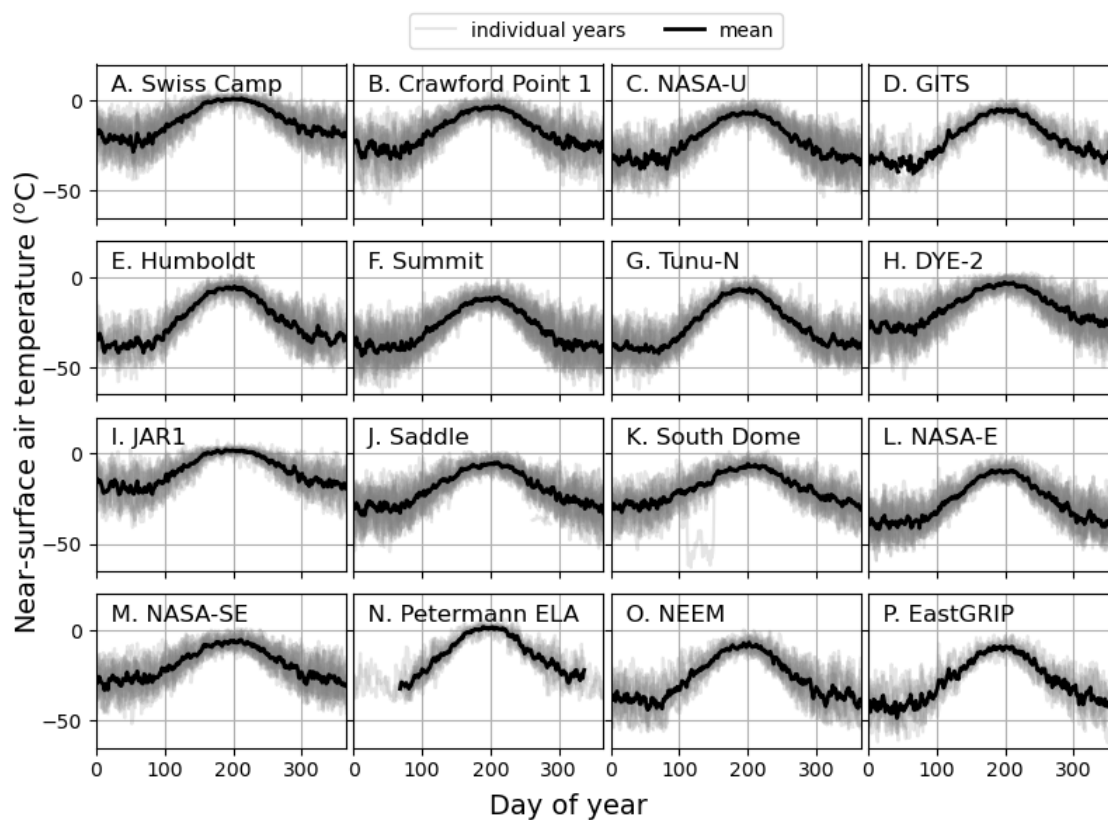
470

Figure 9: Climatology of daily near-surface air temperatures. The interpolated 2 m air temperature is used when the two levels are available, otherwise a single measurement level is used. Climatological values are calculated when at least values for five years are available.

475
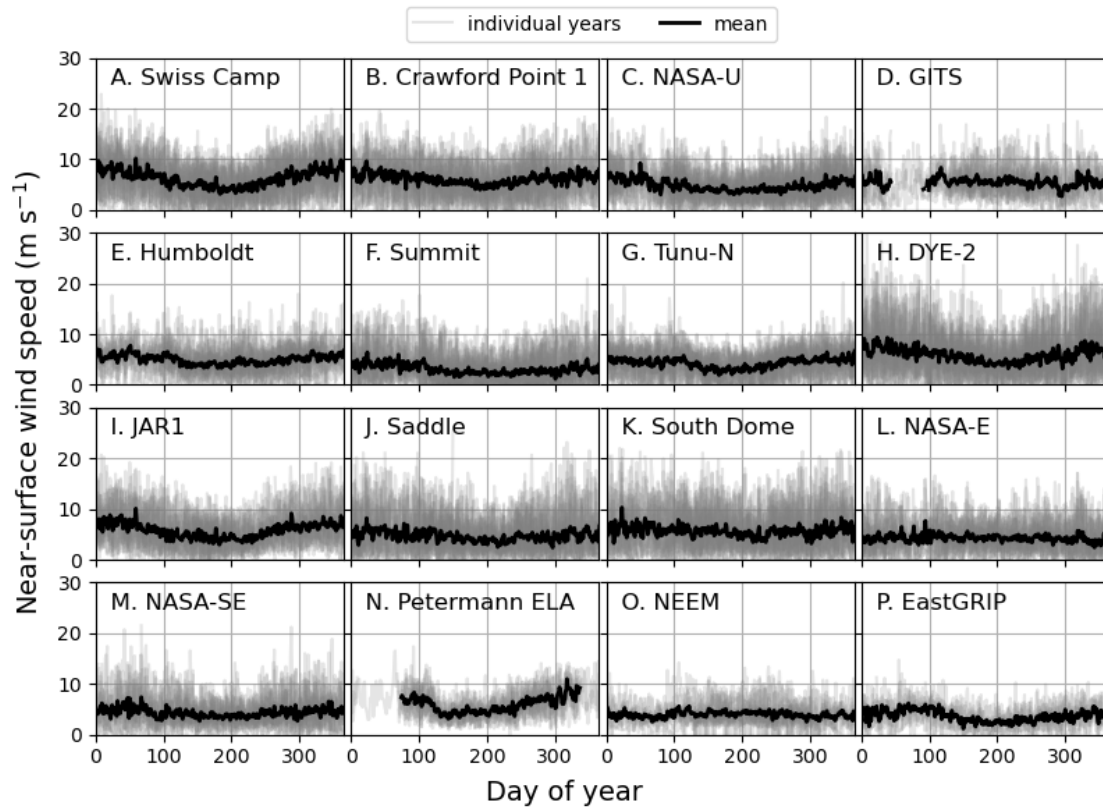
Figure 10: Climatology of the near-surface wind speed. An extrapolated 10 m wind speed is used when the two levels are available, otherwise the available level is used. Climatological values are calculated when at least values for five years are available.

5.4 Dataset evaluation and known limitations

480   With the longevity of some stations (e.g. more than 30 years at Swiss Camp), questions can be raised about the quality and accuracy of the sensors that have been deployed for several years, i.e. sensor drift and deterioration. We here evaluate the air temperature, relative humidity, wind speed, downward and upward shortwave irradiance at nine GC-Net sites relative to independent AWS data during the 2007-2022 period. At Swiss Camp, NASA-E, NASA-U, NEEM, Saddle and DYE-2, the GC-Net data are compared, respectively, to measurements from the SWC, NAE, NAU, NEM AWS installed by GEUS within

485   500 m of the GC-Net stations (GEUS, 2020; How et al., 2022a). DYE-2 data are also compared to measurements from Samimi et al. (2022). The GC-Net station at Summit is compared to the nearby (within 2 km) DMI and NOAA measurements. The metrics presented in Table 4 can be considered as the overall assessment of the relative accuracy and a conservative measurement for the repeatability of the GC-Net data.

490

Table 4. Comparison of the GC-Net AWS data to independent AWS observations at the GC-Net sites. MD stands for mean difference and RMSD for root mean squared difference.

Downward shortwave irradiance (W m^{-2})

GC-Net AWS	Secondary AWS	MD	RMSD
Swiss Camp	SWC	-7.8	41.4
NASA-U	NAU	-21.2	44.0
NASA-E	NAE	-21.0	35.6
NEEM	NEM	-28.6	52.9
Saddle	SDL	-0.3	60.7
DYE-2	U. Calgary	-17.9	60.3
DYE-2	DY2	-6.3	29.5

Reflected shortwave irradiance (W m^{-2})

GC-Net AWS	Secondary AWS	MD	RMSD
Swiss Camp	SWC	-7.3	27.4
NASA-U	NAU	-1.4	16.9
NASA-E	NAE	-24.4	35.0
NEEM	NEM	-9.9	16.7
Saddle	SDL	12.2	47.0
DYE-2	U. Calgary	-5.8	33.7
DYE-2	DY2	-13.2	24.9

Albedo (-)

GC-Net AWS	Secondary AWS	MD	RMSD
Swiss Camp	SWC	0.00	0.06
NASA-U	NAU	0.10	0.11
NASA-E	NAE	-0.02	0.03
NEEM	NEM	0.03	0.07
Saddle	SDL	0.03	0.11
DYE-2	U. Calgary	0.01	0.08
DYE-2	DY2	-0.04	0.06

Air temperature lower (ºC)

GC-Net AWS	Secondary AWS	MD	RMSD
NASA-E	NAE	-0.2	1.0
Summit	NOAA	0.5	2.7

Air temperature upper (ºC)

GC-Net AWS	Secondary AWS	MD	RMSD
Swiss Camp	SWC	0.0	0.4
NASA-E	NAE	-0.2	1.1
EastGRIP	EGP	0.1	0.6
Summit	DMI	0.7	2.3
Summit	NOAA	-2.0	4.0

Surface pressure (hPa)

GC-Net AWS	Secondary AWS	MD	RMSD
Swiss Camp	SWC	3.4	4.0
NASA-U	NAU	-10.6	14
NASA-E	NAE	0.7	0.8
EastGRIP	EGP	0.7	1.7
Saddle	SDL	-0.3	0.6
DYE-2	U. Calgary	-0.3	0.5
Summit	NOAA	0.5	5.3

Relative humidity lower (%)

GC-Net AWS	Secondary AWS	MD	RMSD
Swiss Camp	SWC	8.1	8.8
NASA-U	NAU	-1.7	4.2
NASA-E	NAE	-2.7	5.2
EastGRIP	EGP	-9.5	11.1
DYE-2	U. Calgary	1.7	2.5
Summit	DMI	-1.5	5.4
Summit	NOAA	-4.4	7.9

Relative humidity upper (%)

GC-Net AWS	Secondary AWS	MD	RMSD
NASA-U	NAU	-0.8	3.6
NASA-E	NAE	-3.2	4.7

Wind speed lower (ms^{-1})

GC-Net AWS	Secondary AWS	MD	RMSD
NASA-U	NAU	-1.2	1.4
NASA-E	NAE	-5.5	5.6
NEEM	NEM	-1.9	2.3
DYE-2	DY2	-0.2	0.9

Wind speed upper (ms^{-1})

GC-Net AWS	Secondary AWS	MD	RMSD
Swiss Camp	SWC	0.4	0.7
NASA-U	NAU	-0.4	1.0
NASA-E	NAE	-1.6	1.9
EastGRIP	EGP	-0.3	0.8
Saddle	SDL	-1.1	2.4
Summit	DMI	0.8	2.4
Summit	NOAA	-1.6	2.5

Wind direction lower (º)

GC-Net AWS	Secondary AWS	MD	RMSD
NASA-U	NAU	-47.9	61.7
NEEM	NEM	6.4	45.5
DYE-2	DY2	-4	37.7

Some of the discrepancies between the different AWS measurements in Table 4 are likely due to known limitations of the GC-Net AWS instruments. The GC-Net air temperature measurements were "naturally aspirated", i.e. not ventilated using motorized fans, and therefore subject to solar overheating under low wind speed and high shortwave irradiance (Steffen

and Box, 2001; Box and Steffen, 2001a). Studies in Antarctica have reported temperature differences of up to 8 ºC between ventilated and non-ventilated measurements (Genthon et al., 2011; Morino et al., 2021). However, by comparing the GC-Net measurements to the air temperatures values from actively ventilated instruments on the newer AWS installed at the GC-Net sites (Table 4), we found that this effect can be very site-specific. When comparing 12 collocated pairs of ventilated and unventilated instruments in low wind speed conditions (<2 m s^{-1}) and high downward shortwave irradiance (>200 W m^{-2}), linear correlation between unventilated-to-ventilated temperature difference and downward shortwave irradiance was significant ($P<0.05$) in a minority of 4 cases, while the remaining 8 comparisons showed no significant correlation between temperature difference and downward irradiance.

The hygrometers are sensitive to the harsh conditions on the ice sheet and prone to degradation. Ohmura et al. (1991, 1992) also noted issues with the absolute calibration of the hygrometers installed at Swiss Camp in 1990-1993. The main limitations of hygrometers are their inability to measure supersaturation and the clogging of the porous sensor when the ambient air is saturated or supersaturated, and slow de-clogging when conditions are dry again (Anderson, 1995). Data quality can be judged visually from RH time series, especially in dry and windy regions: the reading will remain constant at 100% with regards to ice and then suddenly dip to more realistic drier values.

The downward and reflected shortwave irradiance measurements, as well as the albedo derived from them, are known to be sensitive to the leveling of the instrument (Wang et al., 2016) and the surface slope (Weiser et al., 2016; Picard et al., 2020). Apart from photogrammetric assessments, which are challenging and from very limited field notes, the tilt of the GC-Net AWS was not measured over the years. Wang et al. (2016) presented the Retrospective, Iterative, Geometry-Based (RIGB) tilt-correction method that estimates the tilt of the station from its measurement of downward shortwave irradiance during clear sky days. Unfortunately, the resource files required by this algorithm (the theoretical downward shortwave irradiance to which the measurements are to be compared) were discontinued after 2015. We have begun working on applying the method to the GC-Net data as part of a future release. Until this correction has been applied, we advise caution when using the radiation and albedo data.

The shortwave irradiance and wind speed measurements are subject to the shadowing of the station. The former when the station's shadow passes over the sensor, for the latter when the anemometer is downwind of the station. These issues were minimized through the design of the station, by installing the pyranometer boom directed south or the anemometers across from the predominant wind direction. Additionally, under certain conditions (e.g., station standing high above the surface), the station mast and logger box may enter the field of view of the pyranometer. Consequently, the AWS may mask part of the diffuse irradiance from the snow. This effect can be corrected, for example on the albedo values in Eq.16 of Aoki et al. (2011), but the exact geometry and tilt of the station is required. This is not pursued here but may be in future data releases.

The type-T thermocouples measuring snow and ice temperature are subject to noise (Cathles et al., 2007, Sampson, 2009). The cause is that thermocouples only measure the temperature difference between a given depth and a reference junction in the logger box and that this reference temperature appeared insufficiently stable, thereby affecting all measurements

synchronously. This synchronous noise does not affect all sites equally and caution is recommended depending on the site and use of these snow and ice temperature data.

Through this review of potential measurement errors, we do our best to highlight potential issues to the data users, especially for applications highly sensitive to data quality. Nevertheless, these errors should be punctual and the majority of the record can be considered as a robust measurement of the surface climate within the uncertainty linked to the sensors (Table 2) and the practical uncertainty found through comparison with other AWS (Table 4).

6 Concluding remarks

The Level 1 reprocessing of the historical GC-Net AWS data brings the GC-Net data to a higher quality standard, distributed under the *FAIR* principles (Wilkinson et al., 2022). This ultimately paves the way to merging these records with data from the modern GC-Net AWS installed by GEUS at the GC-Net sites since 2021. In addition to the iterative procedure of identification and removal of residual erroneous data through an inclusive community effort via the Github issues page, future work is to focus on establishing solar irradiance tilt correction and the study of the long-term effect of firn densification on surface height records.

The GC-Net AWS represent the most widespread and longest consistent meteorological dataset on the Greenland Ice Sheet, with the monitoring sites having reached, or approaching, a climatologically significant time span. The GC-Net data can be used for long-term climate evaluation, but also for process-oriented studies, as ground truth for remote sensing products and regional climate models. These datasets are therefore an essential and valuable asset to assess the response of the Greenland Ice Sheet to a changing climate.

Data and code availability

The stable version of the GC-Net Level 1 dataset is available at https://doi.org/10.22008/FK2/VVXGUT (Steffen et al., 2022). Although many of the AWS have been discontinued, the Level 1 dataset is to be refined through an iterative process of identification and removal of spurious data and potential adjustments of measurements. Updates, i.e. the latest and most refined data are available on the GC-Net-level-1-data-processing repository (Vandecrux et al., 2020). Data users are encouraged to ask their questions and report issues on the issue page of the GC-Net-level-1-data-processing repository. The maintenance reports from the AWS are available at https://doi.org/10.5281/zenodo.7728549 (Vandecrux and Box, 2023) and the fieldwork pictures sorted by site and year are available at https://doi.org/10.5281/zenodo.7839788 (Box et al., 2023b).

The pyNEAD python package is recommended to read and write NEAD files and is archived at https://doi.org/10.5281/zenodo.7728587 (Mankoff and Vandecrux, 2023). For each new release of the Level 1 dataset, the processing scripts will be captured into a code release on the GC-Net-level-1-data-processing repository (Vandecrux et al., 2020). This repository also contains diagnostic plots and codes used to produce Figure 4 and 5. The GPS coordinates inter-

and extrapolation scripts, as well as the plotting code for Figure 7 are available at https://doi.org/10.5281/zenodo.7729070
560 (Vandecrux and Box, 2023b). The scripts used for the evaluation of the GC-Net data against independent AWS and the study of the AWS climatology (Figures 7-8 and Tables 3-4) are available at https://doi.org/10.5281/zenodo.7728938 (Vandecrux, 2023).

Acknowledgments

In addition to the support from several past NASA and NSF grants awarded to K. Steffen (grant nr. NAPW-2158, NAG51-
565 1612, NAG5-10600, NAG5-10857, NNG06GB08G, OPP-9423530), financial support of the 2020 transition came from the DANCEA (Danish Cooperation for Environment in the Arctic) under the Danish Ministry of Energy, Buildings and Climate. The Danish Finance Law currently supports the GC-Net field and data activities. We acknowledge the key contributions from all the people that have participated in the GC-Net project, assisted Konrad Steffen through the years and contributed to the longevity of GC-Net. In particular, we acknowledge (in alphabetical order) the support from Robin Abbott, Waleed Abdalati,
570 Todd Albert, Kate Daniels, Lucia Espona Pernas, Nena Griessinger, Alain Hubert, Russell Huff, Nighat Johnson-Amin, Mike MacFerrin, Molly McCallister, Reza Naderpour, Atsumu Ohmura, Allan Ø. Pedersen, Thomas, Philipps, Gian-Kasper Plattner, Kim Petersen, Martin Proksch, Christian Schneeberger, Christopher Shields, Martina Særrelse, Julienne Stroeve, Benjamin Walter, Øyvind A. Winton and many others.

Author contributions

575 K.S. was leading the GC-Net project, securing funding, maintaining the stations and processing the data until 2020. B.V. coordinated the effort for the reprocessing, compiled the data and metadata and drafted the manuscript. Substantial editing of the text was done by J.E.B., K.D.M., W.I.C., A.R., P.H.. A.P.A., R.S.F. and S.B.A. secured the funding for the visit of the GC-Net sites from 2020. D.A.H., P.H., P.J.W., K.D.M. and M.K.R. contributed to the reprocessing scripts and visualization. I.I.E., R.K.B. and D.H.-A. handled the transmitted data at WSL until 2022. D.A.H., S.Ste., D.M., N.B., N.J.C., M.S., S.Sta., A.H.,
580 B.P., J.W., J.Z., K.Sa., N.P.M. and J.E.B. accompanied and assisted K. S. in the field until 2020. N.B.K., A.R., K.D.M., W.T.C., A.P.A., P.H., B.V. and J.E.B. visited and maintained the GC-Net sites after 2020. All co-author reviewed and approved the manuscript.

Competing interests

B. Vandecrux and K.D. Mankoff are members of the editorial board of Earth System Science Data.

585 **References**

Albert, T.H: Assessment of glacier mass balances from small tropical glaciers to the large ice sheet of Greenland, Ph.D. Thesis, Florida State University, https://doi.org/10.22008/FK2/DQRE71, 2007.

Anderson, P. S.: A Method for Rescaling Humidity Sensors at Temperatures Well below Freezing, Journal of Atmospheric and Oceanic Technology, 11(5), 1388-1391., https://doi.org/10.1175/1520-0426(1994)011<1388:AMFRHS>2.0.CO;2, 1994.

590 Anderson, P. S.: Mechanism for the Behavior of Hydroactive Materials Used in Humidity Sensors, Journal of Atmospheric and Oceanic Technology, 12(3), 662-667., https://doi.org/10.1175/1520-0426(1995)012<0662:MFTBOH>2.0.CO;2, 1995.

Andersen, M.L., Larsen, T.B., Nettles, M., Elosegui, P., Van As, D., Hamilton, G.S., Stearns, L.A., Davis, J.L., Ahlstrøm, A.P., de Juan, J. and Ekström, G.: Spatial and temporal melt variability at Helheim Glacier, East Greenland, and its effect on ice dynamics. Journal of Geophysical Research: Earth Surface, 115(F4). https://doi.org/10.1029/2010JF001760, 2010.

595 Ahlstrøm, A. P., and PROMICE project team: A new programme for monitoring the mass loss of the Greenland ice sheet. GEUS Bulletin, 15, 61–64. https://doi.org/10.34194/geusb.v15.5045, 2008.

Ambach, W.: Untersuchungen zum energieumsatz in der ablationszone des grönländischen inlandeises, expedition glaciologique internationale au Groenland, vol. 4, 63.

Copenhagen, Bianco Lunos Ed., 1977a

600 Ambach, W.: Untersuchungen zum energieumsatz in der akkumulationszone des grönländischen inlandeises, expedition glaciologique internationale au Groenland, vol. 4, 44. Copenhagen, Bianco Lunos Ed., 1977b.

Aoki, T.; Kuchiki, K.; Niwano, M.; Kodama, Y.; Hosaka, M.; Tanaka, T. Physically based snow albedo model for calculating broadband albedos and the solar heating profile in snowpack for general circulation models. J. Geophys. Res. Atmos. 116, https://doi.org/10.1029/2010JD015507, 2011.

605 Aoki, T., Matoba, S., Uetake, J., Takeuchi, N., and Motoyama, H.: Field activities of the "Snow Impurity and Glacial Microbe effects on abrupt warming in the Arctic" (SIGMA) Project in Greenland in 2011-2013. Bulletin of glaciological research, 32, 3-20, https://doi.org/10.5331/bgr.32.3, 2014.

Bales, R. C., McConnell, J. R., Mosley-Thompson, E., and Csatho, B.: Accumulation over the Greenland ice sheet from historical and recent records, J. Geophys. Res., 106(D24), 33813– 33825, https://doi.org/10.1029/2001JD900153, 2001a.

610 Bales, R.C., Mosley-Thompson, E. and McConnell, J.R.: Variability of accumulation in northwest Greenland over the past 250 years. Geophysical Research Letters, 28(14), pp.2679-2682. https://doi.org/10.1029/2000GL011634, 2001b.

Braithwaite, R., Konzelmann, T., Marty, C., and Olesen, O.: Errors in daily ablation measurements in northern Greenland, 1993-94, and their implications for glacier climate studies. Journal of Glaciology, 44(148), 583-588. https://doi.org/10.3189/S0022143000002094, 1998.

615 Bayou, N. and Steffen, K.: QCheck: a Matlab package for the processing of GC-Net automated weather station data, https://github.com/GEUS-Glaciology-and-Climate/GC-Net-Matlab-processing-scripts, Last access 01-03-2023, 2011.

Box, J.E. and Steffen, K.: Sublimation on the Greenland ice sheet from automated weather station observations. Journal of Geophysical Research: Atmospheres, 106(D24), pp.33965-33981, https://doi.org/10.1029/2001JD900219, 2001a.

Box, J.E. and Steffen, K.: FORTRAN and IDL processing scripts for the historical GC-Net data, https://github.com/GEUS-Glaciology-and-Climate/JEB_GC-Net, Last access 01-03-2023, 2001b

Box, J.E, Revheim, M, Vandecrux, B.: GCNet_photogrammetry: GC-Net weather station geometry from field picture photogrammetry (Version v1). Zenodo. https://doi.org/10.5281/zenodo.7729252, 2023a

Box, J.E., Vandecrux, B., Houtz, D., Steffen, K.: GC-Net historical photo archive, Zenodo, https://doi.org/10.5281/zenodo.7839788, 2023b

Box, J. E., Stroeve, J. C., and Abdalati, W.: Steffen K, Abdalati W and Stroeve J (1993) Climate sensitivity studies of the Greenland ice sheet using satellite AVHRR, SMMR SSM/I and in situ data. Meteorology and Atmospheric Physics 51(3–4): 239–258. DOI:10.1007/bf01030497, Progress in Physical Geography: Earth and Environment, 45, 632–638, https://doi.org/10.1177/03091333211011368, 2021.

Bromwich, D. H., Robasky, F. M., Keen, R. A., and Bolzan, J. F.: Modeled Variations of Precipitation over the Greenland Ice Sheet, J. Clim., 6, 1253–1268, https://doi.org/10.1175/1520-0442(1993)006<1253:MVOPOT>2.0.CO;2, 1993.

Brotzge, J. A., and Duchon, C. E.: A Field Comparison among a Domeless Net Radiometer, Two Four-Component Net Radiometers, and a Domed Net Radiometer. J. Atmos. Oceanic Technol., 17, 1569–1582, https://doi.org/10.1175/1520-0426(2000)017<1569:AFCAAD>2.0.CO;2. 2000.

Campbell Scientific: Q-7.1 Net Radiometer, Instruction Manual, https://s.campbellsci.com/documents/us/manuals/q-7-1.pdf, last access February 28 2023, 1996.

Campbell Scientific: SR50 Sonic Ranging Sensor, Instruction Manual, https://s.campbellsci.com/documents/au/manuals/sr50.pdf, last access February 28 2023, 2007.

Cathles, L.M., Cathles, L.M. and Albert, M.R.: A physically based method for correcting temperature profile measurements made using thermocouples. Journal of Glaciology 53(181), 298–304. https://doi.org/10.3189/172756507782202892, 2007.

Citterio, M. ., Mottram, R., Hillerup Larsen, S., and Ahlstrøm, A.: Glaciological investigations at the Malmbjerg mining prospect, central East Greenland. GEUS Bulletin, 17, 73–76, https://doi.org/10.34194/geusb.v17.5018, 2009.

Covi F., Hock R., Reijmer C.H.: Challenges in modeling the energy balance and melt in the percolation zone of the Greenland ice sheet. Journal of Glaciology 1–15. https://doi.org/10.1017/jog.2022.54, 2022.

Cullen, N.J., Mölg, T., Conway, J. and Steffen, K.: Assessing the role of sublimation in the dry snow zone of the Greenland ice sheet in a warming world. Journal of Geophysical Research: Atmospheres, 119(11), pp.6563-6577, https://doi.org/10.1002/2014JD021557, 2014.

Dahl-Jensen, D., Gundestrup, N., Miller, H., Watanabe, O., Johnsen, S., Steffensen, J., et al.: The NorthGRIP deep drilling programme. Annals of Glaciology, 35, 1-4. https://doi.org/10.3189/172756402781817275, 2002.

Fausto, R. S., van As, D., Mankoff, K. D., Vandecrux, B., Citterio, M., Ahlstrøm, A. P., Andersen, S. B., Colgan, W., Karlsson, N. B., Kjeldsen, K. K., Korsgaard, N. J., Larsen, S. H., Nielsen, S., Pedersen, A. Ø., Shields, C. L., Solgaard, A. M., and Box,

J. E.: Programme for Monitoring of the Greenland Ice Sheet (PROMICE) automatic weather station data, Earth Syst. Sci. Data, 13, 3819–3845, https://doi.org/10.5194/essd-13-3819-2021, 2021.

Genthon, C., D. Six, V. Favier, M. Lazzara, and L. Keller: Atmospheric Temperature Measurement Biases on the Antarctic Plateau. *J. Atmos. Oceanic Technol.*, **28**, 1598–1605, https://doi.org/10.1175/JTECH-D-11-00095.1, 2011.

655   Goff, J. A. and Gratch, S.: Low-pressure properties of water-from 160 to 212 °F., Trans. Am. Heat. Vent. Eng., 52, 95–121, 1946.

Greuell, W. and Konzelmann, T.: Numerical modelling of the energy balance and the englacial temperature of the Greenland Ice Sheet. Calculations for the ETH-Camp location (West Greenland, 1155 m asl). Global and Planetary change, 9(1-2), pp.91-114. https://doi.org/10.1016/0921-8181(94)90010-8, 1994.

660   Hahn, L. C., Storelvmo, T., Hofer, S., Parfitt, R., and Ummenhofer, C. C.: Importance of orography for Greenland cloud and melt response to atmospheric blocking, J. Clim., 33, 4187–4206, https://doi.org/10.1175/jcli-d-19-0527.1, 2020.

Hamilton, G. S., and Whillans, I. M.: Point measurements of mass balance of the Greenland Ice Sheet using precision vertical Global Positioning System (GPS) surveys, J. Geophys. Res., 105(B7), 16295– 16301, https://doi.org/10.1029/2000JB900102, 2000.

665   He, F., Clark, P.U.: Freshwater forcing of the Atlantic Meridional Overturning Circulation revisited. Nat. Clim. Chang. 12, 449–454, https://doi.org/10.1038/s41558-022-01328-2, 2022.

Heinemann, G.: The KABEG'97 field experiment: An aircraft-based study of katabatic wind dynamics over the Greenland ice sheet. Boundary Layer Meteorol 93: 75-116, http://doi.org/10.1023/A:1002009530877, 1999.

How, P., Abermann, J., Ahlstrøm, A.P., Andersen, S.B., Box, J. E., Citterio, M., Colgan, W.T., Fausto. R.S., Karlsson, N.B., 670   Jakobsen, J., Langley, K., Larsen, S.H., Mankoff, K.D., Pedersen, A.Ø., Rutishauser, A., Shield, C.L., Solgaard, A.M., van As, D., Vandecrux, B., Wright, P.J.: PROMICE and GC-Net automated weather station data in Greenland, https://doi.org/10.22008/FK2/IW73UU, GEUS Dataverse, V8, 2022a.

How, P., Mankoff, K.D., Wright, P.J., Vandecrux, B.: pypromice, GEUS Dataverse, V1, https://doi.org/10.22008/FK2/3TSBF0, 2022b.The IMBIE Team: Mass balance of the Greenland Ice Sheet from 1992 to 2018. 675   Nature 579, 233–239, https://doi.org/10.1038/s41586-019-1855-2, 2020.

Iosifescu Enescu, I.; Bavay, M.; Mankoff, K. Non-Binary Environmental Archive Data (NEAD) format. EnviDat, https://www.doi.org/10.16904/envidat.187, 2020.

Jensen, C.D.: Weather Observations from Greenland 1958-2021 - Observational Data with Description, DMI Report 22-08, https://www.dmi.dk/fileadmin/Rapporter/2022/DMIRep22-08.pdf, 2022.

680   Kendrick, A. K., Schroeder, D. M., Chu, W., Young, T. J., Christoffersen, P., Todd, J., et al.: Surface meltwater impounded by seasonal englacial storage in West Greenland. Geophysical Research Letters, 45, 10,474– 10,481. https://doi.org/10.1029/2018GL079787, 2018.

Kipp & Zonen, NR Lite 2 Net Radiometer Instruction Sheet, https://www.kippzonen.com/Download/335/Instruction-Sheet-Net-Radiometers-NR-Lite2, Last accessed 28-02-2023, n.d.

685   Konzelmann, T., and Braithwaite, R.: Variations of ablation, albedo and energy balance at the margin of the Greenland ice sheet, Kronprins Christian Land, eastern north Greenland. Journal of Glaciology, 41(137), 174-182. https://doi.org/10.3189/S002214300001786X, 1995.

Kuipers Munneke, P., McGrath, D., Medley, B., Luckman, A., Bevan, S., Kulessa, B., Jansen, D., Booth, A., Smeets, P., Hubbard, B., Ashmore, D., Van den Broeke, M., Sevestre, H., Steffen, K., Shepherd, A., and Gourmelen, N.: Observationally

690   constrained surface mass balance of Larsen C ice shelf, Antarctica, The Cryosphere, 11, 2411–2426, https://doi.org/10.5194/tc-11-2411-2017, 2017.

LI-COR, LI-190SZ Instruction manual, https://www.fondriest.com/pdf/li-cor_190_200_manual.pdf, Last access 01-03-2023, n.d.

Finsterwalder, R.: Expédition Glaciologique Internationale Au Groenland 1957–60 (E.G.I.G.), J. Glaciol., 3, 542–546,

695   https://doi.org/10.3189/S0022143000017299, 1959.

Fristrup, B.: Overvintringsstationer på indlandsisen - III. Amerikanske permanente stationer m.v, Tidsskriftet Grønland, ?, 321–344, 1962.

Matoba, S., Motoyama, H., Fujita, K., Yamasaki, T., Minowa, M., Onuma, Y., Komuro, Y., Aoki, T., Yamaguchi, S., Sugiyama, S., and Enomoto, H.: Glaciological and meteorological observations at the SIGMA-D site, northwestern Greenland

700   Ice Sheet. Bulletin of glaciological research, 33, 7-14, http://doi.org/10.5331/bgr.33.7, 2015.

MacFerrin, M. J., Stevens, C. M., Vandecrux, B., Waddington, E. D., and Abdalati, W.: The Greenland Firn Compaction Verification and Reconnaissance (FirnCover) dataset, 2013–2019, Earth Syst. Sci. Data, 14, 955–971, https://doi.org/10.5194/essd-14-955-2022, 2022.

Mankoff, K. D., Fettweis, X., Langen, P. L., Stendel, M., Kjeldsen, K. K., Karlsson, N. B., Noël, B., van den Broeke, M. R.,

705   Solgaard, A., Colgan, W., Box, J. E., Simonsen, S. B., King, M. D., Ahlstrøm, A. P., Andersen, S. B., and Fausto, R. S.: Greenland ice sheet mass balance from 1840 through next week, Earth Syst. Sci. Data, 13, 5001–5025, https://doi.org/10.5194/essd-13-5001-2021, 2021.

Mankoff, K. and Vandecrux, B.: pyNEAD: Python interface to NEAD file format (Version v1). Zenodo. https://doi.org/10.5281/zenodo.7728587, 2023.

710   McGrath, D., Colgan, W., Bayou, N., Muto, A., and Steffen, K.: Recent warming at Summit, Greenland: Global context and implications, Geophys. Res. Lett., 40, 2091–2096, https://doi.org/10.1002/grl.50456, 2013.

McGrath, D., Bayou, N., and Steffen, K.: Larsen C automatic weather station data 2008–2011, U.S. Antarctic Program (USAP) Data Center. https://doi.org/10.15784/601445, 2021.

Menne, M.J., Durre, I., Vose, R.S., Gleason, B.E., and Houston, T.G.: An overview of the Global Historical Climatology

715   Network-Daily Database. Journal of Atmospheric and Oceanic Technology, 29, 897-910, https://doi.org10.1175/JTECH-D-11-00103.1, 2012.

Morino, S., Kurita, N., Hirasawa, N., Motoyama, H., Sugiura, K., Lazzara, M., Mikolajczyk, D., Welhouse, L., Keller, L. and Weidner, G.: Comparison of Ventilated and Unventilated Air Temperature Measurements in Inland Dronning Maud Land on the East Antarctic Plateau. *J. Atmos. Oceanic Technol.*, **38**, 2061–2070, https://doi.org/10.1175/JTECH-D-21-0107.1, 2021.

720 Mosley-Thompson, E., McConnell, J. R., Bales, R. C., Li, Z., Lin, P.-N., Steffen, K., Thompson, L. G., Edwards, R., and Bathke, D.: Local to regional-scale variability of annual net accumulation on the Greenland ice sheet from PARCA cores, J. Geophys. Res., 106(D24), 33839– 33851, https://doi.org/10.1029/2001JD900067, 2001.

Mosley-Thompson, E., Readinger, C. R., Craigmile, P., Thompson, L. G., and Calder, C. A.: Regional sensitivity of Greenland precipitation to NAO variability, Geophys. Res. Lett., 32, L24707, https://doi.org/10.1029/2005GL024776, 2005.

725 NEEM team: Eemian interglacial reconstructed from a greenland folded ice core, Nature, 493, 489–494, https://doi.org/10.1038/nature11789, 2013

Nerem, R.S., Beckley, B.D., Fasullo, J.T., Hamlington, B.D., Masters, D. and Mitchum, G.T.: Climate-change–driven accelerated sea-level rise detected in the altimeter era. Proceedings of the national academy of sciences, 115(9), pp.2022-2025, https://doi.org/10.1073/pnas.1717312115, 2018.

730 Nishimura, M., Aoki, T., Niwano, M., Matoba, S., Tanikawa, T., Yamasaki, T., Yamaguchi, S., and Fujita, K.: Quality-controlled meteorological datasets from SIGMA automatic weather stations in northwest Greenland, 2012–2020, Earth Syst. Sci. Data Discuss. [preprint], https://doi.org/10.5194/essd-2023-116, in review, 2023.

Noël, B., van de Berg, W. J., Lhermitte, S., and van den Broeke, M. R.: Rapid ablation zone expansion amplifies north Greenland mass loss, Science Advances, 5, eaaw0123, https://doi.org/10.1126/sciadv.aaw0123, 2019.

735 Oerlemans, J., and Vugts, H.F.: A Meteorological Experiment in the Melting Zone of the Greenland Ice Sheet. Bull. Amer. Meteor. Soc., 74, 355–366, https://doi.org/10.1175/1520-0477(1993)074<0355:AMEITM>2.0.CO;2, 1993.

Ohmura, A., Steffen, K., Blatter, H., Greuell, W., Rotach, M., Konzelmann, T., Laternser, M., Abe-Ouchi, A. and Steiger, D.: Energy and mass balance during the melt season at the equilibrium line altitude, Paakitsoq, Greenland ice sheet. ETH Greenland Expedition Prog. Report no. 1, Dept of Geography, Swiss Fed. Inst, of Technol., Zurich, 1991.

740 Ohmura, A., Steffen, K., Blatter, H., Greuell, W., Rotach, M., Konzelmann,T., Forrer, J., Abe-Ouchi, A., Steiger.D., Stober, M. and Niederbàumer, G.: Energy and mass balance during the melt season at the equilibrium line altitude, Paakitsoq, Greenland ice sheet. ETH Greenland Expedition Prog. Report no. 2, Dept of Geography, Swiss Fed. Inst, of Technol., Zurich, 1992.

Oksman, M., Kvorning, A. B., Larsen, S. H., Kjeldsen, K. K., Mankoff, K. D., Colgan, W., Andersen, T. J., Nørgaard-Pedersen,
745 N., Seidenkrantz, M.-S., Mikkelsen, N., and Ribeiro, S.: Impact of freshwater runoff from the southwest Greenland Ice Sheet on fjord productivity since the late 19th century, The Cryosphere, 16, 2471–2491, https://doi.org/10.5194/tc-16-2471-2022, 2022.

Olesen, O. B. and Braithwaite,R.J.: Field stations for glacier-climate research, West Greenland. In Oerlemans.]., ed. Glacier fluctuations and climatic change. Dordrecht, Kluwer Academic Publishers, 207-218, 1989.

750 Olesen, O., and Andreasen, J.-O: Glaciological, glacier-hydrological and climatological investigations around 66°N, West Greenland. Rapport Grønlands Geologiske Undersøgelse, 115, 107–111. https://doi.org/10.34194/rapggu.v115.7842, 1983.

Picard, G., Dumont, M., Lamare, M., Tuzet, F., Larue, F., Pirazzini, R., and Arnaud, L.: Spectral albedo measurements over snow-covered slopes: theory and slope effect corrections, The Cryosphere, 14, 1497–1517, https://doi.org/10.5194/tc-14-1497-2020, 2020.

755 Reeh, N., Thompson, H. H., Higgins, A. K., Weidick, A. and Starzer, W..: Stability conditions of north-east Greenland floating ice margins. In Climate change and sea level: final report of work undertaken for the Commission of the European Communities under contract No. ENV4−CT095−0124, 1 March 1996-28 February 1999 Copenhagen, Danish Polar Center. (Report 9.), 1999.

Reeh, N., O. B. Olesen, H. H. Thomsen, W. Starzer, and C. E. Bøggild, Mass balance parameterisation for Hans Tausen 760 Iskappe, Peary Land, North Greenland, in The Hans Tausen Ice Cap. Glaciology and Glacial Geology, Meddelelser om Grønland, vol. 39, edited by C. U. Hammer, pp. 57--69, Danish Polar Center, Museum Tusculanum Press, 2001.

Rignot, E., and Steffen, K.: Channelized bottom melting and stability of floating ice shelves, Geophys. Res. Lett., 35, L02503, https://doi.org/10.1029/2007GL031765, 2008.

Ridley, J. K., P. Huybrechts, J. M. Gregory, and J. A. Lowe: Elimination of the Greenland Ice Sheet in a High CO2 Climate. 765 J. Climate, 18, 3409–3427, https://doi.org/10.1175/JCLI3482.1, 2005.

Reijmer, C., Kuipers Munneke, P., and Smeets, P.: Helheim firn aquifer weather station data and melt rates, Greenland, 2014–2016. Arctic Data Center. https://doi.org/10.18739/A26D5PB4R, 2019.

Samimi, S., Marshall, S.J., Vandecrux, B. and MacFerrin, M.: Time-domain reflectometry measurements and modeling of firn meltwater infiltration at DYE-2, Greenland. Journal of Geophysical Research: Earth Surface, 126(10), p.e2021JF006295, 770 https://doi.org/10.1029/2021JF006295, 2021.

Sampson, K.: Shallow firn layer climatology derived from greenland climate network automatic weather station data. Master Thesis, Colorado University, https://doi.org/10.13140/RG.2.2.28475.90407, 2009.

Shuman, C. A., Steffen, K., Box, J. E., and Stearns, C. R.: A Dozen Years of Temperature Observations at the Summit: Central Greenland Automatic Weather Stations 1987–99, Journal of Applied Meteorology, 40(4), 741-752. Retrieved Jul 20, 2022, 775 from https://journals.ametsoc.org/view/journals/apme/40/4/1520-0450_2001_040_0741_adyoto_2.0.co_2.xml, 2001.

Sigl, M., Winstrup, M., McConnell, J.R., Welten, K.C., Plunkett, G., Ludlow, F., Büntgen, U., Caffee, M., Chellman, N., Dahl-Jensen, D. and Fischer, H.: Timing and climate forcing of volcanic eruptions for the past 2,500 years, Nature, *523*(7562), pp.543-549, https://doi.org/10.1038/nature14565, 2015.

Simpson, C. J. W.: The British North Greenland Expedition, Geogr. J., 121, 274–289, https://doi.org/10.2307/1790892, 1955.

780 Stearns, C. R., and G. A. Weidner, The polar automatic weather station project of the University of Wisconsin, in International Conference on the Role of the Polar Regions in Global Change: Proceedings of a conference held June 11-15, 1990, at the University of Alaska Fair- banks, vol. 1, edited by G. Weller et al., pp. 58-62, Geophysical Insti- tute, Univ. Alaska, Fairbanks AK, https://inis.iaea.org/collection/NCLCollectionStore/_Public/24/041/24041533.pdf?r=1, 1991.

Steffen, K.: Surface energy exchange at the equilibrium line on the Greenland ice sheet during onset of melt. Annals of
Glaciology, 21, 13-18. https://doi.org/10.3189/S0260305500015536, 1995.

Steffen, K., and deMaria, T.: Surface Energy Fluxes of Arctic Winter Sea Ice in Barrow Strait, Journal of Applied Meteorology
and Climatology, 35(11), 2067-2079. Retrieved Feb 15, 2023, https://doi.org/10.1175/1520-
0450(1996)035<2067:SEFOAW>2.0.CO;2, 1996.

Steffen, K., Box, J. E., and Abdalati, W.: Greenland climate network: GC-Net, in Glaciers, Ice Sheets and Volcanoes: A Tribute
to Mark F. Meier. Ed. S. Colbeck, US Army Cold Regions Reattach and Engineering (CRREL), CRREL Special Report, 98-
103. URL, 1996.

Steffen, K., and Box, J.: Surface climatology of the Greenland Ice Sheet: Greenland Climate Network 1995–1999, J. Geophys.
Res., 106(D24), 33951– 33964, https://doi.org/10.1029/2001JD900161, 2001.

Steffen, K., Cullen, N., Huff, R., Starkweather, S., Albert, T., and McAllister, M..: Variability and forcing of climate
parameters on the greenland ice sheet: greenland climate network (GC-NET), NASA Greenland Progress Report, PDF, 2003.

Steffen, K., Cullen, N. Huff, R., Maurer, J., Stober, M., Hepperle, J., and Heise, A.: Variability and forcing of climate
parameters on the greenland ice sheet: greenland climate network (GC-NET), NASA Greenland Progress Report, URL, 2005.

Steffen, K., Huff, R., Rial, J.: Greenland -accumulation and melt layers: regional climatology, process studies, and seismicity,
NASA Greenland Progress Report, PDF, 2006.

Steffen, K.; Vandecrux, B.; Houtz, D.; Abdalati, W.; Bayou, N.; Box, J.; Colgan, L.; Espona Pernas, L.; Griessinger, N.; Haas-
Artho, D.; Heilig, A.; Hubert, A.; Iosifescu Enescu, I.; Johnson-Amin, N.; Karlsson, N. B.; Kurup Buchholz, R.; McGrath, D.;
Cullen, N.J.; Naderpour, R.; Molotch, N.P.; Pederson, A. Ø.; Perren, B.; Philipps, T.; Plattner, G.K.; Proksch, M.; Revheim,
M. K.; Særrelse, M.; Schneebli, M.; Sampson, K.; Starkweather, S.; Steffen, S.; Stroeve, J.; Watler, B.; Winton, Ø. A.; Zwally,
J.; Ahlstrøm, A.: GC-Net Level 1 automated weather station data, https://doi.org/10.22008/FK2/VVXGUT, GEUS Dataverse,
V3, 2023.

Stroeve, J., Box, J.E., Wang, Z., Schaaf, C. and Barrett, A.: Re-evaluation of MODIS MCD43 Greenland albedo accuracy and
trends. Remote Sensing of Environment, 138, pp.199-214, https://doi.org/10.1016/j.rse.2013.07.023, 2013.

Thomas, R., Akins, T., Csatho, B., Fahnestock, M., Gogineni, P., Kim, C., Sonntag, J.: Mass Balance of the Greenland Ice
Sheet at High Elevations. Science, 289(5478):426-428. https://doi.org/10.1126/science.289.5478.426. 2000 .

Thomas, R. H.: Program for Arctic Regional Climate Assessment (PARCA): Goals, key findings, and future directions, J.
Geophys. Res., 106(D24), 33691– 33705, https://doi.org/10.1029/2001JD900042, 2001.

Thomsen, H. H., N. Reeh, O. B. Olesen, W. Starzer, and C. E. Bøggild, Bottom melting, surface mass balance and dynamics
of floating North-East Greenland ice tongues, Final report, EC Environment and Climate Programme 1994-1998, Copenhagen,
1999

Toniazzo, T., Gregory, J.M., and P. Huybrechts, P.: Climatic Impact of a Greenland Deglaciation and Its Possible
Irreversibility. J. Climate, 17, 21–33, https://doi.org/10.1175/1520-0442(2004)017<0021:CIOAGD>2.0.CO;2, 2004.

Van As, D.: Warming, glacier melt and surface energy budget from weather station observations in the Melville Bay region of northwest Greenland. Journal of Glaciology, 57(202), 208-220, https://doi.org/10.3189/002214311796405898, 2011.

Van As, D., Bøggild, C. E., Nielsen, S., Ahlstrøm, A. P., Fausto, R. S., Podlech, S., and Andersen, M. L.: Climatology and ablation at the South Greenland ice sheet margin from automatic weather station observations, The Cryosphere Discuss., 3, 117–158, https://doi.org/10.5194/tcd-3-117-2009, 2009.

Van den Broeke, M.R., Duynkerke, P.G. and Oerlemans, J.: The observed katabatic flow at the edge of the Greenland ice sheet during GIMEX-91. Global and Planetary Change, 9(1-2), pp.3-15. https://doi.org/10.1016/0921-8181(94)90003-5, 1994.

van den Broeke, M., D. van As, C. Reijmer, and R. van de Wal: Assessing and Improving the Quality of Unattended Radiation Observations in Antarctica. J. Atmos. Oceanic Technol., 21, 1417–1431, https://doi.org/10.1175/1520-0426(2004)021<1417:AAITQO>2.0.CO;2, 2004.

Vandecrux, B.: GC-Net evaluation scripts (Version v1). Zenodo. https://doi.org/10.5281/zenodo.7728938, 2023.

Vandecrux, B., Box, J., Houtz, D., and Revheim, M. K. The GC-Net level 1 dataset and processing scripts, https://github.com/GEUS-Glaciology-and-Climate/GC-Net-level-1-data-processing, Last access: 01-03-2023, 2023a.

Vandecrux, B., Houtz, D., Box, J.E.: GC-Net historical metadata compilation [Data set]. Zenodo, https://doi.org/10.5281/zenodo.7728549, 2023b.

Vandecrux, B. and Box, J.E.: GC-Net AWS observed and estimated positions (Version v1) [Data set]. Zenodo. https://doi.org/10.5281/zenodo.7729070, 2023c.

Van de Wal, R.S.W. and Russell, A.J.: A comparison of energy balance calculations, measured ablation and meltwater runoff near Søndre Strømfjord, West Greenland. Global and Planetary change, 9(1-2), pp.29-38. https://doi.org/10.1016/0921-8181(94)90005-1, 1994.

Wang, W., Zender, C. S., van As, D., Smeets, P. C. J. P., and van den Broeke, M. R.: A Retrospective, Iterative, Geometry-Based (RIGB) tilt-correction method for radiation observed by automatic weather stations on snow-covered surfaces: application to Greenland, The Cryosphere, 10, 727–741, https://doi.org/10.5194/tc-10-727-2016, 2016.

Weidner, G. A., and C. R. Stearns, A Two-Year Record of the Climate on the Greenland Crest from an Automatic Weather Station, in International Conference on the Role of the Polar Regions in Global Change: Proceedings of a conference held June 11-15, 1990, at the University of Alaska Fair- banks, vol. 1, edited by G. Weller et al., pp. 58-62, Geophysical Insti- tute, Univ. Alaska, Fairbanks AK, 1991.

Weidner, G., King, J., Box, J.E., Colwell, S., Jones, P., Lazzara, M., Cappelen, J., Brunet, M. and Cerveny, R.S.: WMO evaluation of northern hemispheric coldest temperature: −69.6 °C at Klinck, Greenland, 22 December 1991. *Q J R Meteorol Soc*. 147: 21– 29. https://doi.org/10.1002/qj.3901, 2020.

Weiser, U., Olefs, M., Schöner, W., Weyss, G., and Hynek, B.: Correction of broadband snow albedo measurements affected by unknown slope and sensor tilts, The Cryosphere, 10, 775–790, https://doi.org/10.5194/tc-10-775-2016, 2016.

Wilkinson, M., Dumontier, M., Aalbersberg, I. et al. The FAIR Guiding Principles for scientific data management and stewardship. Sci Data 3, 160018. https://doi.org/10.1038/sdata.2016.18, 2016.

Zender, C., Wang, W., Laffin, M. and Saini, A.: JAWS: An extensible toolkit to harmonize and analyze polar automatic weather station datasets. University of California, Irvine. PDF https://github.com/jaws/jaws 2018.